ASTROBIOLOGY
Volume 2, Number 2, 2002

Research Paper

Remote Sensing of Planetary Properties and Biosignatures on Extrasolar Terrestrial Planets

DAVID J. DES MARAIS,[1] MARTIN O. HARWIT,[2] KENNETH W. JUCKS,[3] JAMES F. KASTING,[4] DOUGLAS N.C. LIN,[5] JONATHAN I. LUNINE,[6] JEAN SCHNEIDER,[7] SARA SEAGER,[8] WESLEY A. TRAUB,[3] and NEVILLE J. WOOLF[6]

ABSTRACT

The major goals of NASA's Terrestrial Planet Finder (TPF) and the European Space Agency's Darwin missions are to detect terrestrial-sized extrasolar planets directly and to seek spectroscopic evidence of habitable conditions and life. Here we recommend wavelength ranges and spectral features for these missions. We assess known spectroscopic molecular band features of Earth, Venus, and Mars in the context of putative extrasolar analogs. The preferred wavelength ranges are 7–25 μm in the mid-IR and 0.5 to ~1.1 μm in the visible to near-IR. Detection of O_2 or its photolytic product O_3 merits highest priority. Liquid H_2O is not a bioindicator, but it is considered essential to life. Substantial CO_2 indicates an atmosphere and oxidation state typical of a terrestrial planet. Abundant CH_4 might require a biological source, yet abundant CH_4 also can arise from a crust and upper mantle more reduced than that of Earth. The range of characteristics of extrasolar rocky planets might far exceed that of the Solar System. Planetary size and mass are very important indicators of habitability and can be estimated in the mid-IR and potentially also in the visible to near-IR. Additional spectroscopic features merit study, for example, features created by other biosignature compounds in the atmosphere or on the surface and features due to Rayleigh scattering. In summary, we find that both the mid-IR and the visible to near-IR wavelength ranges offer valuable information regarding biosignatures and planetary properties; therefore both merit serious scientific consideration for TPF and Darwin. Key Words: Spectroscopy—Biosignatures—Extrasolar planets—Terrestrial Planet Finder—Darwin—Habitable planets. Astrobiology 2, 153–181.

[1]Ames Research Center, Moffett Field, CA.
[2]Cornell University, Ithaca, NY.
[3]Harvard–Smithsonian Center for Astrophysics, Cambridge, MA.
[4]Pennsylvania State University, State College, PA.
[5]University of California, Santa Cruz, CA.
[6]University of Arizona, Tucson, AZ.
[7]Observatoire de Paris, Meudon, France.
[8]Institute for Advanced Study, Princeton, NJ.

WHY CONDUCT A SPECTROSCOPIC SEARCH FOR LIFE IN THE COSMOS?

OUR SEARCH FOR LIFE elsewhere will inevitably deepen our understanding of life itself. Current definitions of life usually enumerate its key properties (e.g., Morowitz, 1992). For example, they cite the ability of cells and ecosystems to harvest energy, metabolize, replicate, and evolve. Our definitions are based upon life on Earth, yet they will affect our strategy to search for life elsewhere. Accordingly, we must distinguish between attributes of life that are truly universal versus those that solely reflect the particular history of our own biosphere. Herein we assume that all life requires complex organic compounds that interact in a liquid water solvent. These assumptions do not seem overly restrictive, given that life is an information-rich entity that depends fundamentally upon the strong polarity of its associated solvent. Carbon compounds and structures appear to be unrivaled in their potential for attaining high information contents. Other plausible solvents cannot match the strong polar–nonpolar dichotomy that water maintains with certain organic substances, and this dichotomy is essential for maintaining stable biomolecular and cellular structures. However, our own biosphere utilizes only a small fraction of the number of potentially useful organic compounds. Alien life forms probably explored alternative possibilities, and so their discovery will increase the known diversity of life.

A spectrum of opinion exists concerning the extent to which the origin and evolution of life on Earth were directed (deterministic) processes or were more random (driven by contingency) (Des Marais and Walter, 1999). One view holds that chance might play a role, but only within limits set by the physical and chemical properties of life (DeDuve, 1995). While evolution on another planet might have explored alternative paths, " . . . certain directions may carry such decisive selective advantages as to have a high probability of occurring elsewhere as well . . ." (DeDuve, 1995). An alternative view is that the process of evolution might reflect the outcome principally of an infinite number of "contingent" events (Gould, 1996). Thus if we were able to "rewind the tape of life and replay it," we would get a fundamentally different result every time. One major barrier to resolving these divergent views is that we know the history of only one biosphere. If we had other examples, we could directly compare them and begin to discern general principles of the origins and evolution of life. This circumstance creates a powerful scientific argument to look for life elsewhere.

How might we search for inhabited extrasolar planets? The detection *in situ* of life is a strategy that might be viable within the Solar System, but not for extrasolar planets. However, it seems feasible to detect biological signatures, or "biosignatures," by remote sensing. There are at least two types of biosignatures: spectral and/or polarization features created by biological products and electromagnetic signals created by technology. The latter example of a biosignature requires SETI-like searches. However, this discussion addresses spectral signatures of biological products, as well as properties of habitable planets. These are indeed promising targets for near-term exploration (e.g., Owen, 1980). Spectral biosignatures can arise from organic constituents (e.g., vegetation) and/or inorganic products (e.g., atmospheric O_2). Spectral features originating from a planet's surface are likely to be localized in specific regions, whereas gaseous biosignatures can become globally distributed by atmospheric circulation.

BASIC SCIENCE GOALS IN THE SEARCH FOR SPECTRAL SIGNATURES OF EXTRASOLAR LIFE, AND THE BROAD DIVERSITY OF TERRESTRIAL PLANETS

Within our own Solar System, the search for extraterrestrial life and evidence about the origin of earthly life will likely be confined to Mars, Europa, and Titan. Small bodies such as comets, asteroids, and meteorites offer insights concerning chemical "building blocks" for the origins of life. Such objects present a wonderful opportunity for detailed studies that is not possible when we make explorations outside the Solar System. But, the compensating advantages of studies beyond the Solar System are the greater diversities of both planetary environments and their stages of development that are available for investigation. The search for extrasolar planets with biospheres, what we will refer to here as habitable planets, is a search for the broadest biological diversity possible—a search for planets bearing life whose origin almost certainly is independent of our own, given the enormous distances and harsh radiation of interstellar space.

In determining the appropriate wavelength range in which to detect spectroscopically the characteristics of a habitable world, one must bear in mind that the range of characteristics of rocky planets is likely to exceed our experiences with the four terrestrial planets and the Moon. While the nearly (but not quite) airless Moon and Mercury arguably represent the lifeless end-member case of terrestrial planets, there are always surprises. For example, Mercury appears, based on radar data, to support small polar caps of water ice, and the origin of the water appears to be exogenic impact of icy material followed by molecular migration to the poles. Were such a body to be in a planetary system in which the orbital plane happens to be face-on to the Earth, could that water ice signature be detectable in the near-IR range, and, if so, what would one conclude about the habitability of such an object? Habitability might be ruled out if the semimajor axis were too small (indeed, the planet might be missed altogether), but no laws of physics rule out a "Mercury" placed at the orbit of, say, Venus (0.7 AU). What would one conclude then?

Likewise, absent Jupiter in our planetary system, a rather water-rich terrestrial planet, possibly with a mass comparable to Earth's, might have formed in place of Mars, or beyond Mars in the orbital region of our present asteroid belt. We have absolutely no experience with such a body, and models of the stability of a dense greenhouse atmosphere and surface-atmosphere evolution are our only guides to such a case. What signatures would we look for in the case of such an object? How would we determine whether signs of habitability suggest equable conditions over geologic time versus, say, limited periods in the distant or even recent past, except by assumption?

In some systems, planets may not be coplanar, and thus the orbits of any terrestrial planets might slowly migrate in and out of the habitable zone over long periods of time. Likewise, Earth-like planets orbiting stars of very different spectral type than the Sun, hence of different spectral energy distribution, might evolve differently. Other planets will differ from Earth in the relative amounts of UV versus visible flux that they receive from their parent star, in the variability of the parent star's luminosity over time, and in the characteristics of the stellar wind and the star's magnetosphere. Such differences translate into a diversity of patterns of atmospheric evolution and planetary habitability that are, unfortunately, hard to quantify.

The ill-fated protagonist of Shakespeare's play *Hamlet* admonished his friend that: "There are more things in Heaven and Earth, Horatio, than are dreamt of in your philosophy." Today we might instead warn ourselves of the certainty that there are more kinds of Earths in the heavens than are dreamt of in our philosophy. Any mission to detect and characterize spectroscopically terrestrial planets around other stars must be designed so that it can characterize diverse types of terrestrial planets with a useful outcome. Such missions are now under study—the Terrestrial Planet Finder (TPF), by NASA, and Darwin, by the European Space Agency. Because the designs of these two missions are far from being finalized, we do not distinguish between their potential capabilities, but simply refer for convenience to the concept of a large space-borne spectroscopic mission for characterizing terrestrial planets and detecting life as TPF/Darwin in what follows.

The principal goal of TPF/Darwin is to provide data to the biologists and atmospheric chemists. These investigators will evaluate the observations of a potentially broad diversity of objects in terms of evidence of life and the environmental conditions in which such life would be present (e.g., Beichman *et al.*, 1999; Caroff and Des Marais, 2000). The TPF/Darwin concept hinges on the assumption that one can screen extrasolar planets for habitability spectroscopically. For such an assumption to be valid, we must answer the following questions: What makes a planet habitable, and how can that be studied remotely? What are the diverse effects that biota might exert on the spectra of planetary atmospheres? What false-positives might we expect? What are the evolutionary histories of atmospheres likely to be? And, especially, what are robust indicators of life? The search strategy should include the following goals that collectively serve as milestones for the development of TPF/Darwin.

TPF/Darwin must survey nearby stars for planetary systems that include terrestrial-sized planets in their habitable zones ["Earth-like" planets (Beichman *et al.*, 1999)]. Through spectroscopy, TPF/Darwin must determine whether these planets have atmospheres and establish whether they are habitable. We define a habitable planet in the "classical" sense, meaning a planet having an atmosphere and with liquid water on its surface. The habitable zone therefore is that zone within which light from the planet's parent star (its "Sun") is sufficiently intense to maintain

liquid water at the surface, without initiating runaway greenhouse conditions that dissociate water and sustain the loss of hydrogen to space (Kasting *et al.*, 1993). The size of a planet can determine its capacity to sustain habitable conditions (e.g., Kasting *et al.*, 1993). Larger planets sustain higher levels of tectonic activity that also persists for a longer time. Tectonic activity sustains volcanism and also heats crustal rocks and recycles CO_2 and other gases back into the atmosphere. These outgassing processes are required to ensure climate stability over geologic timescales (Kasting *et al.*, 1984).

There are interesting potential examples where liquid water might exist only deep below the surface, such as the Jovian moon Europa (e.g., Reynolds *et al.*, 1987) or on present-day Mars. However, biospheres for which liquid water is present only in the subsurface might not be detectable by TPF/Darwin. Thus a planet having liquid water at its surface meets our operational definition of habitability, which is that habitable conditions must be detectable. Studies of planetary systems will also reveal how the abundances of life-permitting volatile species such as water on an Earth-like planet are related to the characteristics of the planetary system as a whole (Lunine, 2001).

TPF/Darwin data will allow targeting of the most promising planets for more detailed spectroscopy to detect biosignatures. A biosignature is a feature whose presence or abundance requires a biological origin. Biosignatures are created during the acquisition of the energy or the chemical ingredients that are necessary for biosynthesis or both (e.g., leading to the accumulation of atmospheric oxygen or methane). Biosignatures can also be products of the biosynthesis of information-rich molecules and structures (e.g., complex organic molecules and cells). Life may be indicated by chemical disequilibria that cannot be explained solely by nonbiological processes. For example, a geologically active planet that exhales reduced volcanic gases can maintain detectable levels of atmospheric oxygen only in the presence of oxygen-producing photosynthetic organisms. Alternatively, an inhabited planet having a moderately reduced interior might harbor greater concentrations of atmospheric methane than an uninhabited planet, owing to the biosynthesis of methane from carbon dioxide and hydrogen at cooler ($<120°C$) temperatures (Committee on the Origin and Evolution of Life, 2002).

Although the "cross hairs" of the TPF/Darwin search strategy should be trained upon "Earth-like" planets, TPF/Darwin should also document the physical properties and composition of a broader diversity of planets. This capability is essential for the proper interpretation of potential biosignature compounds. For example, the presence of molecular oxygen in the atmospheres of Venus and Mars can indeed be attributed to nonbiological processes, but only through a proper assessment of the conditions and processes involved (e.g., Kasting and Brown, 1998). On the other hand, a planet might differ substantially from Earth yet still be habitable. Accordingly, in order to assess thoroughly the cosmic distribution of habitable planets, we must understand both the processes of formation of planetary systems as well as the controls upon the persistence of habitable zones. This approach ultimately calls for observations of multiple planets within systems, including those that are uninhabitable. A strategy that seeks not only Earth-like planets but also the context required for habitable planetary systems (Kasting, 1988) to develop will probably lead us most directly to that first evidence that we are not alone in the Universe.

The present paper uses a spectroscopic model of Earth, along with other planetary data, to assess promising wavelength regions and spectral features for the screening of habitable from uninhabitable planets and for the characterization of planetary environments. Specifically, the question of the relative promise of the optical versus the IR spectrum is crucial to mission design, and is quantitatively addressed here. This paper also provides useful algorithms for the analysis of spectral features relevant to the question of a planet's habitability. Following a discussion of the interpretation of visible and IR spectra of the terrestrial planets of our own Solar System, the spectrum of the atmospheres of terrestrial planets is separated by IR and visible molecular band features into key components—gases, such as water, carbon dioxide, and oxygen compounds, and clouds. Our knowledge of the spectral signature of terrestrial planet surfaces, known and putative, is discussed, and finally the recommendations for TPF/Darwin programs based on the analyses of the earlier sections are summarized.

This presentation should be viewed as an assessment of the current state of the art for the remote spectroscopic detection of habitable planets and life. Just as recent conceptual and technological breakthroughs have revolutionized modern

astronomy, we anticipate that future developments will indeed revolutionize our search for life elsewhere.

INTERPRETATION OF VISIBLE AND IR SPECTRA OF TERRESTRIAL PLANETS

The simple observation that a planet exists at some distance from a star will determine whether the planet is in a predefined habitable zone of the star (which may or may not delineate where life is possible), but it in fact only provides a very rough estimate of the temperature. There are two temperatures of interest: the effective temperature (that of a blackbody having the same surface area and the same total radiated thermal power) and the surface temperature (defined to be that at the interface between any atmosphere and the solid surface). In general, if there is a greenhouse effect present (e.g., from CO_2, H_2O, CH_4, or aerosols), then the surface temperature will be warmer than the effective temperature. The effective temperature is determined by the stellar brightness, the distance, R, to the star, the albedo, A, and whether the annually averaged day–night temperature difference at the radiating level ($\Delta T_{\text{D-N}}$) is small (as for a rapidly rotating planet or a planet with a massive atmosphere) or large (as for a slow rotator or a thin atmosphere). Our own Solar System offers the following examples:

Venus: $R = 0.72$ AU, $A = 0.80 \pm 0.02$ (Tomasko, 1980), $\Delta T_{\text{D-N}}$ is small

Earth: $R = 1.00$ AU, $A = 0.297 \pm 0.005$ (Goode *et al.*, 2001), $\Delta T_{\text{D-N}}$ is small

Mars: $R = 1.52$ AU, $A = 0.214 \pm 0.063$ (Kieffer *et al.*, 1977), $\Delta T_{\text{D-N}}$ is large

If we assume that we have a planet within this range of values, but with otherwise unknown specific values of R, A, and $\Delta T_{\text{D-N}}$, then the predicted effective temperatures will span a range of 202K, which is almost uselessly large. If we assume that we know precisely R, A, or $\Delta T_{\text{D-N}}$, then the predicted range drops to 123, 159, or 169, respectively, showing that the most important parameter is R, followed by A, and finally $\Delta T_{\text{D-N}}$. If we know R from physical observations with TPF/Darwin, then the range of possible effective temperatures drops to 123K, which is still rather large. Finally, assuming that we know at least two of these parameters, the range falls to 75K if we know $\Delta T_{\text{D-N}}$, and 70K if we know A. Of course, if we know all three parameters the uncertainty falls formally to 0. The actual uncertainties will always be larger when the error bars in the measurements are taken into account.

By definition, we can determine A if we measure both the visible and IR flux, which immediately argues in favor of a TPF/Darwin design capable of observing in both parts of the electromagnetic spectrum. We can determine $\Delta T_{\text{D-N}}$ by either of two methods. We can measure the IR flux at two or more points in the orbit (looking at the day and night sides, respectively), or we can measure the visible flux at two or more points in a diurnal cycle of a planet with discernible surface features to indicate rotation rate. These methods work perfectly if the observer is near the orbital plane, and badly if the observer is near the orbital pole.

Regarding the search for life, constraining a planet's surface temperature holds much greater value than constraining the effective temperature. For example, both Venus and Earth have similar effective temperatures (220K and 255K, respectively), but vastly different surface temperatures (730K and ~290K, respectively), owing to the divergent greenhouse gas column abundances. Visible and/or IR spectra can help interpret these cases, but neither is able to penetrate clouds; therefore surface conditions may well be difficult to estimate.

However, other important attributes of the planet can be discerned from spectra. Given the spectrum of an extrasolar planet, it is possible to derive the physical conditions and aspects of the composition at the layer where the optical depth is near unity, at the wavelength of observation. IR observations of the continuum give a color temperature. By equating this with the physical temperature, we can derive the planet size from the IR emission, but IR spectral band profiles are strongly affected by the details of the thermal structure of the atmosphere. Hence, while these spectral bands can be used to tell the presence or near absence of atmospheric constituents and to constrain the thermal structure, they are poorly suited for determining quantitative abundances.

The visible/near-IR continuum can yield a definite relationship between size and the planet's reflectivity (albedo) in the visible and near-IR. Properties of individual bands can allow inference of planet size, albedo, and temperature. The intensities of visible/near-IR absorption features

are not affected by thermal structure; therefore they are suitable for abundance determinations, but they are a much less direct measure of a planet's temperature than is the thermal IR part of the spectrum. The combination of IR and visible observations is of course most valuable: Neither region will yield all of the information, and either region will require modeling to interpret.

There is, however, a concern that Earth is a peculiarly easy planet to interpret from external observations. Planets that differ in their size, insolation, or land–ocean fraction may well have more cloud cover and be much harder to interpret for that reason, as was the case for early studies of Venus (Cruikshank, 1983). Ultimately, additional observations with very large space interferometers at millimeter wavelengths will probably be needed to determine surface temperatures of cloudy planets, while those with significant clear patches should have surface conditions discerned by a visible-IR TPF/Darwin system. However, synthesis of model spectra and extraction of temperatures for model planets, as well as observing programs using the planets of our own Solar System as test objects, are needed so that reliable extraction of surface temperatures of extrasolar planets can be assured.

Observations across interstellar distances can only distinguish those planets whose habitability is apparent from observations of the reflected or emitted radiation. Planets with habitable surfaces that are hidden by deep, totally opaque atmospheres, or with only a small fraction of the surface exposed to view, probably cannot be recognized as habitable. We are limited to exploring habitability for only those planets that are habitable on a global scale and that have mostly clear atmospheres in a significant part of the optical or IR spectrum, or both. Since the occurrence of habitable planets, relative to the total number of stars that possess planetary systems, is presently unknown, we allow ourselves to make the error of assuming a planet uninhabitable when it is in fact habitable or inhabited. We are more concerned about making the other type of error—that is, to conclude that a planet is habitable or inhabited when in fact it is not.

The surfaces of planets hidden by opaque clouds could be studied at wavelengths long enough to penetrate the clouds. In practice, this requires observations in the far-IR or millimeter wavelength ranges. For extrasolar planets, this cannot be achieved with current technology because it would require interferometric reflectors having very large diameters and baselines. On the other hand, if the surface temperature can be determined, then wavelengths that do not penetrate to the surface can be used to distinguish surface characteristics from features observed at some higher level in the atmosphere. If the observable upper levels of the troposphere, corresponding to where the temperature falls with altitude from the surface upward, appear to be moderately close to saturation with water vapor, it is possible to determine approximate characteristics at ground level. To do this, one must assume that the atmosphere is in convective equilibrium with a wet adiabat. On the other hand, if one can only observe the stratosphere because of an optically thick photochemical smog, it is essentially impossible to extrapolate from stratospheric conditions down to the surface. Both Venus and Titan are totally enshrouded by photochemical clouds, and close-flyby spacecraft and *in situ* techniques have been required to determine the conditions in their lower atmospheres and at their surfaces (Lindal *et al.*, 1983; Seiff, 1983). Furthermore, because it is possible to have an atmospheric layer of low humidity above a layer of high humidity associated with a permanent atmospheric temperature inversion (e.g., the stratosphere above the tropopause on Earth), it is not possible to conclude that a dry upper atmosphere implies a dry surface.

Cloud coverage on any given planet depends on the atmospheric structure, composition, and circulation patterns. While larger bodies tend to have denser atmospheres and more cloud, distance from the parent star also matters: witness Mercury versus Titan, similar-sized bodies. Of the two larger terrestrial planets in our system, one is roughly half cloud-covered (Earth), and the other is completely cloud-covered (Venus). For small and intermediate cloud coverage, the surface characteristics can be found fairly well. For extensive clouds, we can only determine the characteristics of the cloud layer and above. It is not yet clear whether cloud cover that is sustained by convective processes typically produces an atmosphere having extensive regions that are cloud-free, but at least two Solar System objects (Earth and Jupiter) exhibit such behavior.

In what follows we will consider the information on an extrasolar planet that can be gained from IR and visible spectra, respectively, by themselves and then in combination. We shall

start by considering information available from the continuum and proceed from there to spectral bands.

Continuum observations

We first attempt to determine the planet's orbit, so as to estimate the insolation, or energy input per unit area. Both visible and IR measurements can give the projected orbit. From this it should be possible to infer the true orbit. Even without that, it should be possible to determine the maximum elongation, and with the assumption of a circular orbit this elongation is a direct measure of the planet–star separation. With that information, we know the insolation and can utilize observations of the spectral continuum to determine how the thermal environment of the planet compares with corresponding Solar System planets.

Continuum observations also can be used to estimate planetary radii and masses (see below). As explained earlier (see Basic Science Goals in the Search for Spectral Signatures of Extrasolar Life, and the Broad Diversity of Terrestrial Planets), these properties are also important to know because they provide clues to a planet's formation history, its ability to retain an atmosphere, and its ability to foster life.

It is straightforward to estimate planetary radius from the measured mid-IR flux. From observations in the mid-IR wavelength range, we can expect to measure a color temperature from spectral shape. That temperature may be a temperature of the surface, of low clouds, or of high clouds. By equating color temperature for selected spectral regions with physical temperature and using the observed flux, we can use Planck's Law to obtain the surface area, and hence radius, of the planet. To infer the likely planet mass we can use the observed Solar System relationship among mass, radius, and thermal environment. Although we have considered that the presence of rings or satellites might distort our answer, we expect IR continuum observations to determine the planet radius to an accuracy of ~10%.

With the size and temperature, we can calculate the total surface emission, and compare it with the insolation. That comparison will tell us the Bond albedo (Eqs. 1 and 2). Let r_{pl} = planet radius (unknown), A = albedo (unknown), D = distance to planetary system, L^* = star integral flux at Earth, θ = angle of planet maximum elongation, T = observed color temperature, $F(\lambda)$ = observed thermal planet flux at wavelength λ, and $B(\lambda,T)$ = Planck function at wavelength λ for temperature T. Then we have

$$(r_{pl}/D)^2 = F(\lambda)/\pi B(\lambda,T) \quad (1)$$

and

$$1 - A = [(D/r_{pl})^2\ \theta^2\ 4\int F(\lambda)\ d\lambda]/L^* \quad (2)$$

From albedo we can tell whether the cloud cover of the planet resembles that of the Moon, Mars, Earth, or Venus. However, in the past, the Earth has been through a cold phase in which it had a high albedo (owing to ice) and a low surface temperature. We could not distinguish such a snowball Earth from a Venus-like planet from albedo alone; spectra would be required to distinguish water ice from sulfuric acid droplets. Absent spectra, if the albedo were high, we would know that either we were determining cloud-top characteristics or we were seeing an ice-bound planet. If the albedo were low, it would seem likely that we were seeing a surface, and determining surface characteristics. If the albedo were intermediate, we could expect that we were underestimating the surface temperature, but not badly.

At visible and near-IR wavelengths, a planet's radius and mass might be estimated from the planet's apparent brightness or colors. The Solar System provides a framework within which to develop methods for making such estimates. Gas giant and terrestrial-sized planets can be easily distinguished by their apparent brightness (a function of area, albedo, and phase) and orbital distance. Considering the surface area ratio of Jupiter to Earth and assuming the same albedo, Jupiter would be 120 times brighter than the Earth at the same orbital distance. Unless giant planet albedos are 10–100 times smaller than terrestrial-sized planet albedos, confusion between giant and terrestrial-sized planets is unlikely. By using a rough estimate of radius from the apparent brightness and assuming some density, the "photometric mass" can be constrained. Alternatively, planet mass might be estimated from low-resolution photometry, yielding a "color mass" (so-called by analogy with color temperature in the IR). The key idea is that a planet's color can indicate whether it is a giant or terrestrial type, based on our experience with the particular spec-

tral properties of the planets and atmospheres in our Solar System, as discussed below.

While our Solar System provides a good template for interpreting brightness and color mass, a much greater diversity of planets is likely and challenges their use for estimating planetary radii and masses. For example, Earth has had very different signatures throughout geologic time. The postulated "snowball Earth" during the Neoproterozoic Eon would have had a very high albedo (Hoffman *et al.*, 1998). Earth's atmosphere might have contained a larger methane component during the Archean Eon [prior to 2.5 billion years ago (Kasting and Brown, 1998)] and therefore exhibited extremely strong methane spectral features. Another exception to the Solar System template is an icy Uranus just at the outer border of the habitable zone. Strong deviations from Solar System gas giant spectral signatures also are expected for young, hot Jupiters. Despite expected uncertainties, photometric mass and color mass together hold promise for providing estimates of planet mass.

The surface temperature of a terrestrial planet can be determined from IR observations only under a very limited range of conditions. For present Earth, one could obtain it moderately well, in principle, by making observations in the 8–12 μm "window" region. However, there is some absorption by the wings of water vapor bands in the window region even at present. If the surface temperature were to increase moderately, the water abundance would increase substantially, and, eventually, the surface would no longer be seen, even in this window region. The observed emission would then come from a region that is located several water scale heights higher in the atmosphere. This would yield a measured temperature that is substantially lower than the actual surface temperature. Thus for planets much warmer than Earth, the surface temperature cannot be determined by IR observations. And, of course, such a warm condition could precipitate a catastrophic greenhouse conversion from an Earth-like to a Venus-like condition.

Alternatively, if we consider a more massive planet than Mars, but receiving Mars-like insolation, the surface temperature will only be Earth-like if the planet's greenhouse effect is much larger than that of Earth, in which case, again, the surface temperature will likely not be available to IR observations. Or, if we have a small planet with a thin atmosphere but receiving a Venus-like insolation, then a moist planet will develop a blackbody temperature of ~300K, and with greenhouse warming, the amount of water in the atmosphere will likely make the surface temperature indeterminate.

An oxygen feature under either of these circumstances cannot be interpreted as a definitive sign of life because oxygen having a nonbiological origin can accumulate on a large ice-bound planet (Des Marais, 1997; Kasting, 1997). The ice prevents it from being absorbed by the surface rock. However, a larger planet is likely to have volcanoes and volcanic exhalations with chemical compositions that are reducing and therefore would remove any nonbiological oxygen inventories. Therefore there may be only a very small range of planetary conditions that might produce a false-positive answer for oxygen. Nonbiological oxygen might also become apparent on a hot planet undergoing a catastrophic greenhouse conversion (Kasting, 1988). As the atmosphere is warmed, the tropopause temperature stays fixed, but the tropopause moves up to high altitudes where the pressure is low (Ingersoll, 1969). Thus, the saturation water vapor mixing ratio, which is equal to the vapor pressure divided by the ambient pressure, becomes high. The stratosphere becomes wet, and water vapor attains high altitudes where it is easily dissociated, hydrogen is lost, and oxygen retained until it reacts with surface rock. However, Earth's tropopause is at 210K, cold enough to keep the stratosphere quite dry at the altitudes where water is exposed to substantial UV fluxes. This too might give a false-positive answer for the detection of life. Both of these conditions are distinguishable by the planet being outside the habitable zone; therefore we can probably discriminate between real and false-positives.

In summary, the first and best-known aspect of a planet from IR observations is its size. From the size, insolation, and integrated emission we can determine both the albedo and a temperature associated with the emitting layer. It may be possible from these three parameters to understand whether the region being observed is close to ground or a layer high in the atmosphere. If it is an upper layer, interpretation of surface characteristics is sometimes possible, but there are clearly cases where it is not.

Observations of bands

Molecular band observations at low resolution are most informative regarding the abundances

of materials. The strength of bands varies with both the amount of material and the atmospheric pressure. For likely planets, the breadth of individual lines in the band will vary linearly with the pressure, but the absorption from a given line will vary with the square root of the abundance of material. A curve of growth (which is the relationship between the abundance of a species and the intensity of one of its bands) will, over most of its range, satisfy a relationship that the band strength is proportional to the pressure as well as the square root of the column abundance of the gas. In such a relationship, pressure-induced self-broadening is about twice as effective as broadening by another gas. These two quantities cannot be separated unless the atmospheric pressure is very low, and Doppler broadening dominates. This circumstance will only occur for weak spectral bands in the visible region. (The pressure broadening is directly related to the frequency of collisions of molecules, whereas Doppler broadening is proportional to the line frequency, which will be greatest in the visible.) For this reason it will in general be hard to quantify precisely the meaning of an observed band strength in terms of abundances.

It is even harder to interpret the strength of a band in the mid-IR spectral range. There the absorbing material also emits. An absorption band exhibits a steadily higher opacity towards its center. Thus the band profile actually indicates the vertical temperature structure above the continuum-emitting region. Some features, such as central inversion or absence of inversion, may be informative about the vertical temperature structure in the atmosphere. Thus, for example, the central inversion in the 15 μm band of CO_2 on Earth is caused by the temperature increase from tropopause to stratosphere, which, in turn, is caused by O_3 absorbing sunlight. Such information could, for example, actually confirm that O_3 were indeed present.

Absorption by water poses an interesting challenge for interpretation. Water absorption is observed in the near-IR spectra of cool giant stars and brown dwarfs. The bands are the same as those seen in Earth's spectrum, but they are somewhat broader, and therefore they modify the apparent shape of the continuum between bands. The bands imply a certain value for the product of pressure and the square root of the water abundance. The water could be saturated if abundant enough, which is a rather nonspecific statement since the vapor pressure varies from the freezing point to the boiling point by a factor of ~180. Thus a fairly precise measure of temperature is needed to take advantage of information about the strength of water bands.

The widths of water and oxygen features hardly increase with temperature, and therefore cannot be used to infer temperature. It is more likely that water band strengths can be used to determine an approximate range of temperatures and pressures. The amount of water is established by vapor pressure, and so there is probably some lower limit to temperature implied by keeping the atmospheric pressure reasonable. These relationships need investigation.

In the mid-IR range, the short wavelength end of the rotational continuum overlaps with the long wavelength end of the 15 μm CO_2 band. Therefore the observed quantity is the depth of drop at this long wavelength edge. It gives information about the temperature where the water opacity is roughly unity as seen from above. If we assume a saturated atmosphere, then, the lower the atmospheric pressure, the less will be the difference in temperature between the short and long wavelength edges of this band. The relationship between the band feature and the estimate of temperature, made from observations of the continuum, must be investigated further. Such observations might provide estimates of pressure as well at levels in the atmosphere where the water band is observable.

Determining parameters from visible and near-IR bands

In addition to the bands, it is necessary to start with an approximate determination of the planet size. The visual luminosity of the planet and its annual phase variation can be used to derive the quantity $A(r_{pl})^2$. We require g, the acceleration due to gravity at the planet surface.

Let ρ be the planet mean density:

$$g = 4/3Gr_{pl}\pi\rho \tag{3}$$

We can assume $\rho \sim 5$ as a first approximation for a terrestrial planet. So g only varies with the square root of A. That is, it is uncertain by a factor of about ± 1.7.

There are two kinds of molecules: ones that vary in mixing ratio (H_2O and O_3) and ones that have constant mixing ratio. For the gases having

constant mixing ratios and that produce bands, we can use oxygen and carbon dioxide to estimate the total pressure, under the assumption that the mixing ratio is unity (that is, we assume that we have a pure O_2 or CO_2 atmosphere). This will give a lower limit to the pressure at the surface of view. And, because the gas pressure varies linearly with T, we can assume some mean T ~260K (a reasonable approximation for Earth, Venus, or Mars), from the fact that we have chosen to study only planets in the potentially habitable zone.

For H_2O, we must assume the scale height (for terrestrial temperatures, it is about one-fifth the atmospheric scale height because of condensation). Thus using the just-determined surface pressure and the H_2O band strength we can determine the vapor pressure of water at the surface. This can then be translated into a better temperature by assuming that the atmosphere is 50% saturated. Then this temperature can be fed back into the pressure determination, and the process iterated.

It would be advisable to use this process to test against observations of Earth, Mars, and Venus as well as simulations of a "smaller" Venus and "larger" Mars to explore the quality of the results. Indeed, it is a necessary step in this work that both visible and IR processes be validated.

Effects of dust rings, binary planets, and dust trails

The derivation of the albedo A of a planet from its radius r_{pl} and reflected flux, $F_r = A\pi r_{pl}^2\phi(t)$ [where $\phi(t)$ is an orbital phase factor], assumes that the planet is spherical. That assumption is not true if either there are circumplanetary rings and/or the planet possesses a companion. The latter case can involve a satellite that is smaller than the planet, as with Earth, Jupiter, and Saturn. However, the diversity of planetary systems that has already been discovered leaves open the possibility that some extrasolar planet companions may be as large as the planet itself ("binary planets"); the Pluto–Charon pair in the Solar System nearly qualifies. Although the lifetime of rings may be short (10^4 years), one cannot exclude that they are continuously replenished. In these two cases, the planetary albedo that is estimated from its reflected flux (or its radius derived from an estimated or "guess" albedo) will be incorrect. "Countermeasures" have been proposed that address these potential sources of error (Schneider, 1999).

These issues are presented more thoroughly elsewhere (Des Marais *et al.*, 2001). Here we briefly summarize key results. Planet-trailing dust clouds were discussed by Beichman *et al.* (1999). For the cloud like the one that is currently believed to trail the Earth, the flux is ~10% of that of the Earth. However, in systems having much more dust, the dust would compromise IR observations as well as visible imaging at low angular resolution after apodization.

Observations in the visible range can distinguish between the effects of rings versus effects of binary planets or moons. Rings will likely express a distinctive shape in their phase effect. Eclipses might possibly reveal moons and binary planets. Such information would be helpful in determining the parameters of a moon–planet system.

In the mid-IR range, the effects of a terrestrial-sized moon would be relatively unimportant, but a larger moon would result in spectral features whose strength varied throughout the year, and its temperature similarly would appear to vary in this cycle. A planet in an eccentric orbit would show the temperature variation, but not the washing out of spectral features. High-precision positional measurements that are performed as part of the study of planets might help to discriminate between the various effects and to infer a planet's mass.

Summary

We have examined the potential use of both visible/near-IR spectra and mid-IR spectra to interpret observations of terrestrial planets at both wavelengths. Estimates of planet size and albedo can definitely be determined from mid-IR observations. These parameters are more difficult to determine from visible observations, but iterative schemes can be developed for exploring this, and methods that utilize either wavelength range should be tested against actual observations and models.

Surface temperature determination is only possible if there is a planet with a substantial fraction that is cloud-free. The presence of O_2 and H_2O is determinable from both spectral regions, but care will be needed to exclude false-positives (e.g., Selsis *et al.*, 2002) where detection of O_2 and O_3 is not a sign of life.

IR AND VISIBLE MOLECULAR BAND FEATURES

In this section we go beyond the general considerations outlined above to synthesize specific spectral features of key molecular gases expected in terrestrial planet atmospheres, under the temperature, pressure, and compositional conditions of the Earth. The resulting library of spectral features should provide a useful and quantitative starting point for modeling of equivalent features identified in the light from extrasolar terrestrial planets. For readers not familiar with spectral line analysis, standard textbooks in the field should be consulted (Goody and Yung, 1989).

Model

Model Earth spectra are calculated with the Smithsonian Astrophysical Observatory (SAO) code originally developed to analyze balloon-borne far-IR thermal emission spectra of the stratosphere, and later extended to include visible reflection spectra (Traub and Stier, 1976; Traub and Jucks, 2002). The spectral line database includes the large Air Force Geophysical Laboratory compilation plus improvements from prerelease Air Force Geophysical Laboratory material and other sources. In a few cases, laboratory data are available but spectroscopic analysis is not, so here we use an empirical, so-called pseudo-line band shape. The far wings of pressure-broadened lines can be non-Lorentzian at around 1,000 times the line width and beyond; therefore, in some cases (H_2O, CO_2, N_2) we replace line-by-line calculation with measured continuum data in these regions. Dust and Rayleigh scattering are approximated by applying empirical wavelength power laws that exert an appreciable effect in the visible blue wavelength range. Atmospheres from 0 to 100 km altitude are constructed from standard models that are discretized to appropriate atmospheric layers, and additional radiative transfer methods are used to ensure that line cores and optically thick layers are accurately represented. Integration over the spherical Earth's atmosphere is approximated to a few percent accuracy by a single-point calculation at a zenith angle of 60°, so the effective air mass is 2 in the IR (outgoing emission) and 4 in the visible (2 incoming sunlight plus 2 outgoing reflected light). Clouds are represented by inserting continuum-absorbing/emitting layers at appropriate altitudes, and broken clouds are represented by a weighted sum of spectra using different cloud layers.

In Fig. 1 we show a simple model (Traub and Jucks, 2002) of spectra from the Sun and Solar System planets as seen from 10 pc, about the distance of a typical nearby star. This model assumes blackbody continuum spectra at the effective temperature of each object, plus reflectance spectra proportional to the visible albedo of each planet. The zodiacal light component is appropriate to a 0.1 AU diameter patch centered at 1.0 AU from the central star. The molecular band absorption features for the Earth's atmosphere have been superimposed for reference. No attempt has been made to model non-blackbody features, such as the strong Rayleigh scattering from Earth, molecular features of the other planets, or wavelength-dependent albedos.

In Fig. 2 we show the IR portion of the model Earth spectrum as seen from 10 pc. The band features and the cloud models will be discussed at length in the following sections. Figure 3 shows the visible to near-IR portion of the model Earth spectrum, with the same cloud models included. The purpose of Figs. 1–3 is to show the model spectra in physical units, which can easily be converted into photon count rates, for example. All subsequent figures will show spectra in relative units of emissivity in the IR or relative reflectivity in the visible to near-IR, so as to emphasize the spectroscopy as opposed to the photometric flux at each wavelength.

What follows are graphical and descriptive results for each atmospheric feature or species, in both the mid-IR and visible-near-IR spectral ranges.

Clouds (Figs. 4 and 5)

The IR model Earth spectrum in Fig. 4 illustrates the combined effects of spectral absorption features and clouds. The clear-atmosphere spectrum (cloud-free) is shown by the uppermost curve, illustrating that, with no clouds, we can penetrate deepest into the troposphere and therefore observe the warmest (brightest) emitting altitudes. If the planet is covered with high clouds, at about the altitude of the tropopause, we get the lowest curve, which is essentially a blackbody at the tropopause temperature, plus superimposed emission features from the higher-altitude warmer layers in the stratosphere. The

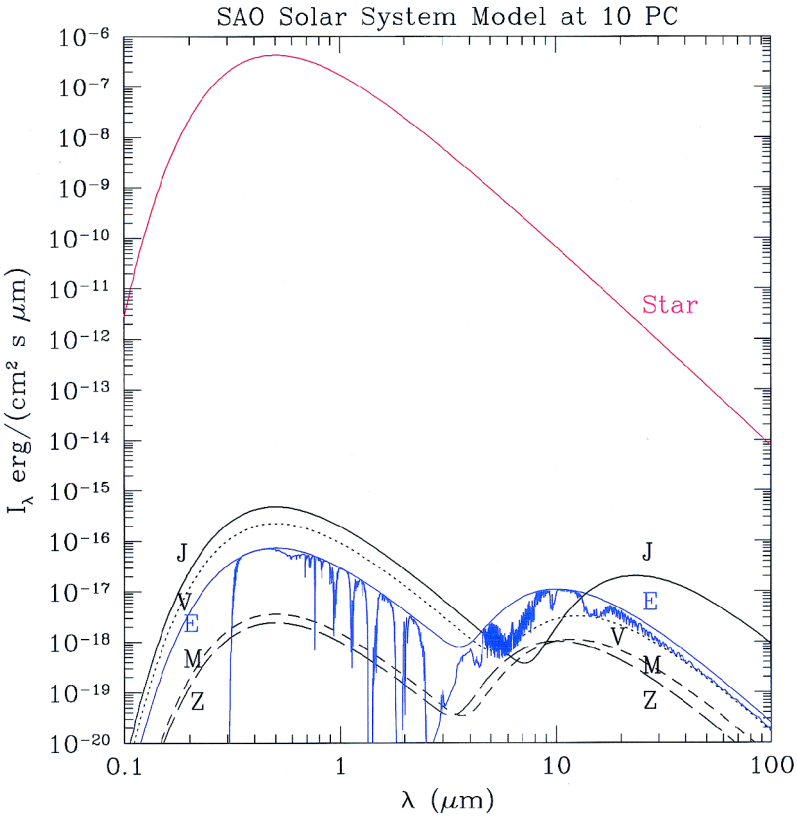

FIG. 1. Model spectrum of the sun and planets as seen from a distance comparable to that of a nearby star (10 pc), shown in physical units. Simple Planck emission and wavelength-independent albedo reflectance components are shown. For Earth, a pure molecular absorption spectrum is superimposed for reference.

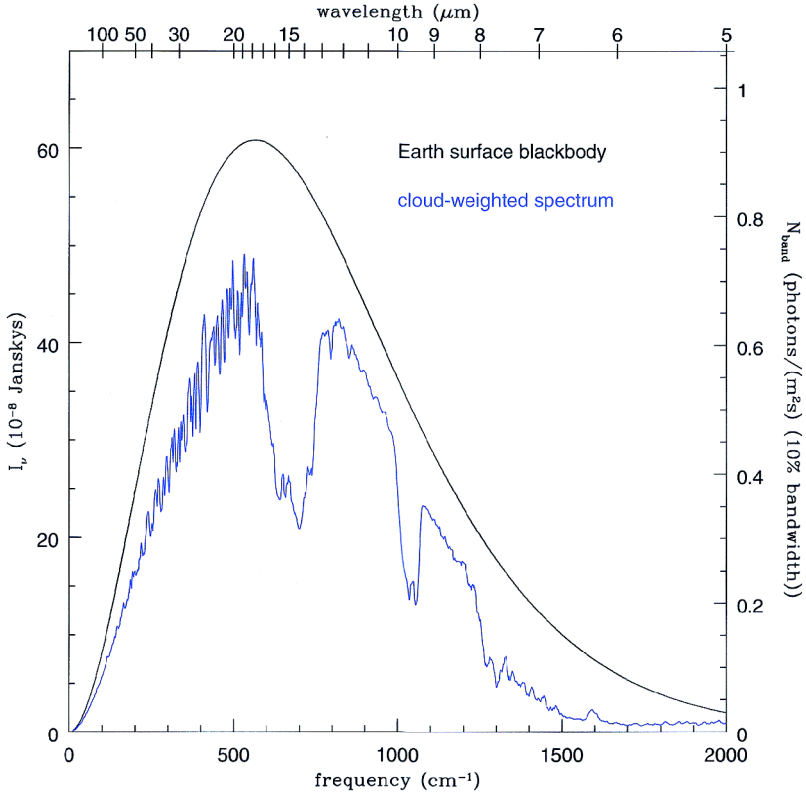

FIG. 2. IR portion of the Earth model spectrum, showing the blackbody spectrum of the Earth's surface in the absence of an atmosphere (upper curve) and the net spectrum after the addition of the dominant atmospheric molecular species and a realistic model atmosphere mixed in with a model distribution of opaque clouds distributed over several altitudes (lower curve). Two intensity scales are provided: astrophysical units (left) and photons (right).

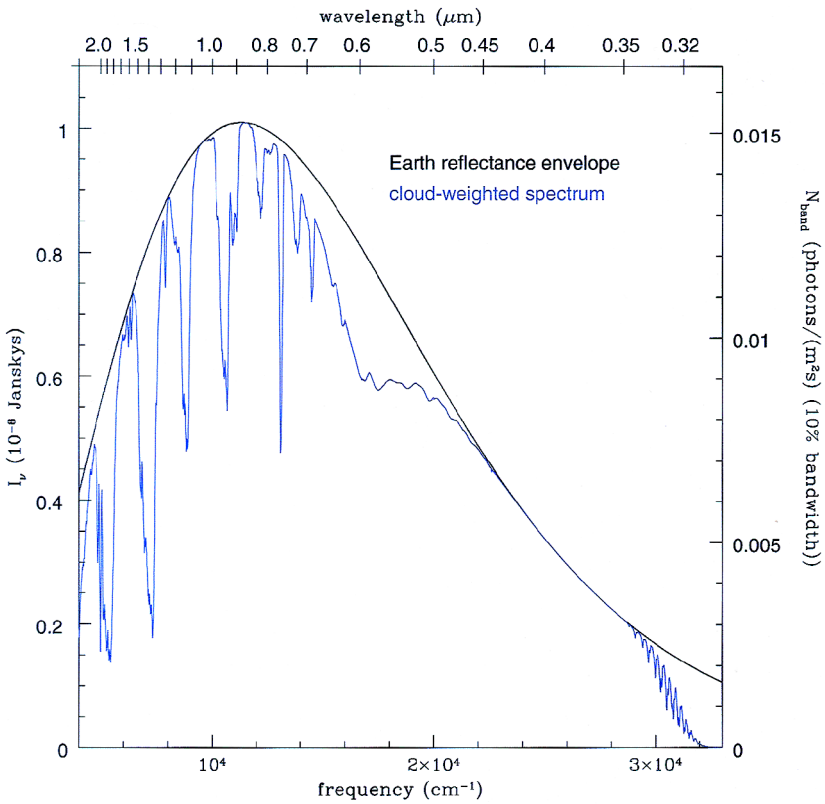

FIG. 3. Visible and near-IR portion of the Earth model spectrum, showing a reflection spectrum of the Earth's surface and clouds in the absence of an atmosphere (upper curve) and the net spectrum after the addition of the dominant atmospheric molecular species and a realistic model atmosphere mixed in with a model distribution of opaque clouds distributed over several altitudes (lower curve). Two intensity scales are provided: astrophysical units (left) and photons (right).

curves in between these two extreme cases show intermediate-altitude cloud covers. The heavy (middle) curve represents the combined effect of a weighted average of clear and cloudy patches to simulate roughly the present Earth. This range of spectra shows that clouds and gas species may dominate the mid-IR spectrum. All IR spectra are triangle-smoothed to a resolution (wavelength over wavelength interval) of 25.

The model Earth spectrum for the visible range, in Fig. 5, shows five curves representing spectra from the surface, then from each of three cloud layers, and a weighted average of these components. Because the clouds are assumed to be the same at all wavelengths, their main effect is to make the absorption lines appear less deep. The visible spectra are smoothed to a resolution of 100 using a triangle function.

Water (Figs. 6 and 7)

Water has a present atmospheric level (PAL) of ~8,000 ppm, corresponding to ~50% relative humidity at the 288K model surface. Water vapor is concentrated in a few-kilometer layer near its liquid water source at the surface, falls to a minimum of a few parts per million at the tropopause, and increases to ~6 ppm in the stratosphere. Water in the stratosphere is produced both by upward transport from the troposphere and by oxidation of methane that also is tropospheric in origin. The optical depth increases approximately as the square root of abundance, because most water lines are saturated. The abundance of H_2O increases exponentially with temperature, but it is independent of ambient pressure. Thus the information that we derive from the H_2O bands is a mixture of the surface H_2O availability, surface temperature, vertical mixing activity, vertical temperature profile, and photochemical reactions.

The mid-IR spectrum of H_2O is shown in Fig. 6. The upper curve is for zero water abundance (0 ppm) and is of course a flat line, because here we have an atmosphere-free planet and we see down to the 288K surface. The main features are the rotational bands (~15 μm and longer wavelength) and vibrational bands (~5–8 μm). Adding tropospheric H_2O produces opacity at altitudes above the ground, hence cooler molecular kinetic temperatures and lower emitted flux levels, and thus the spectral features that appear to be absorption features are actually simply emission from lower-temperature layers of the atmosphere. Four potential bands are indicated where the assumed extremes of wavelength are set by

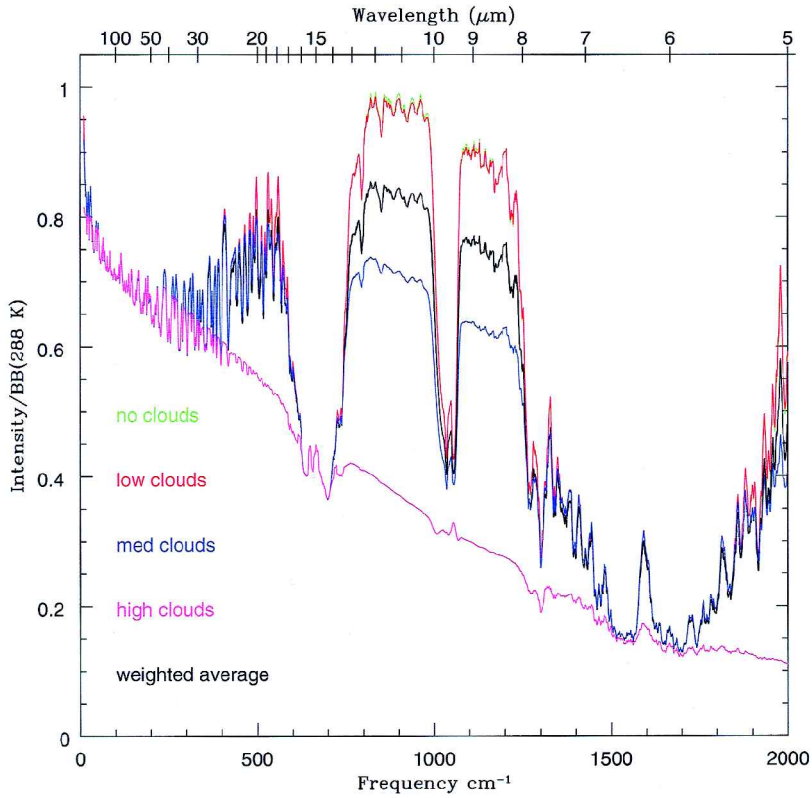

FIG. 4. Normalized IR thermal emission spectral models of the Earth are shown for five cloud conditions. Each spectrum is calculated as discussed in the text, for the present Earth's altitude-dependent, midlatitude temperature structure and gas species mixing ratio profiles, and at a zenith angle of 60° to simulate closely a whole Earth integration. Frequency (in wavenumbers, cm^{-1}) is indicated at the bottom, and wavelength (in μm, 10^{-6} m) as marked at the top. Each spectrum is normalized to a blackbody (BB) spectrum at 288K. A convenient way to interpret these spectra is to note that, at each wavelength, the emitted flux is that of a BB at a temperature that corresponds to the atmospheric temperature at an altitude where the optical depth is unity, where the optical depth is computed along a path from the top of the atmosphere downwards. For example, in the 20–100 μm region, the rotational band of water is so strong that we only see radiation from the relatively cold upper troposphere and not from the hot surface or lower troposphere. The top curve represents a cloud-free atmosphere, with spectral features as explained in subsequent figures. The other curves represent complete overcast conditions with clouds at low, medium, and high altitudes, plus a curve for a nominally realistic mixture of these four cases. The weighted average spectra have cloud altitudes and covering fraction as follows: low cloud, 1 km, 20%; medium cloud, 6 km, 30%; and high cloud, 12 km, 10%. In the IR spectrum, the main effect of adding clouds is to decrease the emitted continuum flux and reduce (and potentially invert) the relative depths of spectral features.

instrumental spatial resolution at long wavelengths and by the weakness of emitted flux at short wavelengths. The best features may be the 17–50 μm rotational bands, which give information on water in the stratosphere as well as troposphere. The 6–7 μm region may be a second choice, since CH_4 and N_2O can overlap this region.

The visible spectrum of H_2O is shown in Fig. 7. The spectrum shows relatively equally spaced bands that are very strong at long wavelengths and weaker at short wavelengths. In the 0.5–1.0 μm interval alone, there are five significant H_2O features with a range of band strengths. Although H_2O tends to dominate the visible spectrum, it does so in discrete bands that happened to be centered at wavelengths such that most other species are still accessible. On an Earth-like planet, the H_2O features in the 0.7, 0.8, and 0.9 μm regions are good candidates for detection. The strong, longer wavelength bands in the 1.1, 1.4, and 1.9 μm areas are excellent candidates if this region were instrumentally accessible.

Carbon dioxide (Figs. 8 and 9)

CO_2 has a PAL of 355 ppm, uniformly mixed. The IR spectrum (Fig. 8) shows both the target

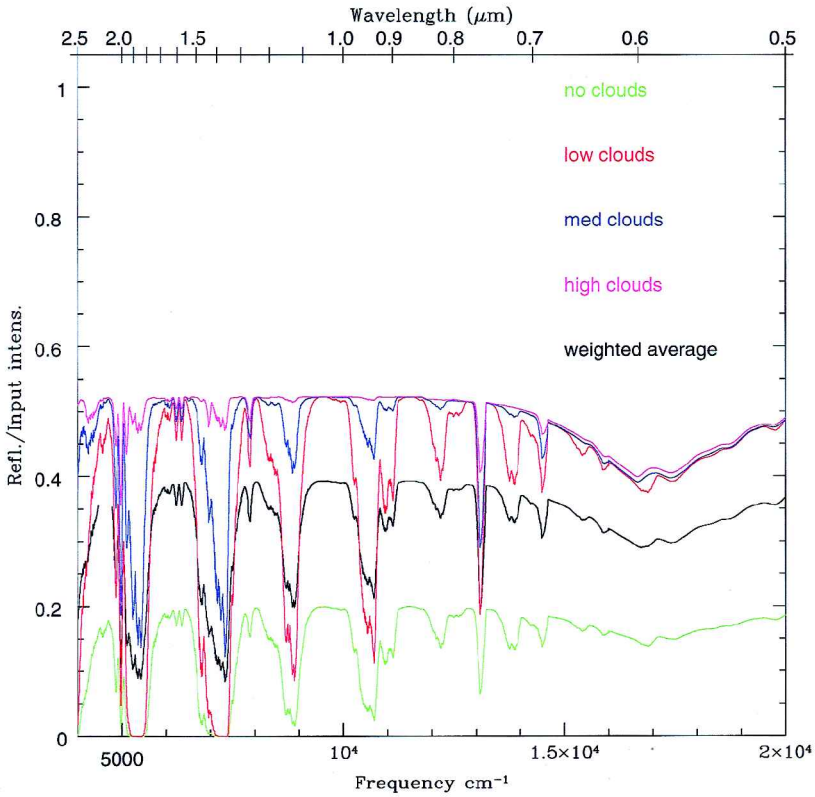

FIG. 5. Normalized visible reflection spectral models of the Earth, for the same model atmosphere and cloud conditions as shown in Fig. 4. The clear atmosphere case in the lower curve has the smallest continuum level owing to the fact that the surface reflectivity is low compared with clouds, and conversely the overcast cloud cases have high continuum fluxes. The weighted average is a linear combination of the extreme cases and was calculated for an overall albedo of ~39%, which is higher than the most recently available value of ~29.7% (Goode *et al.*, 2001). The weighted average spectra have cloud altitudes and covering fraction as follows: low cloud, 1 km, 20%; medium cloud, 6 km, 30%; and high cloud, 12 km, 10%. In the reflected spectrum, the main effect of adding clouds is to increase the reflected continuum flux and reduce the relative depths of absorption features.

species and also a background spectrum due to the present-Earth H_2O abundance. We believe that including the spectrum for H_2O provides a useful element of practicality because H_2O may well be a dominant spectral contributor. The main CO_2 band is centered at 15 μm, and it is so strong that it is saturated for all mixing ratios shown. The central reversal in the 15 μm band at high

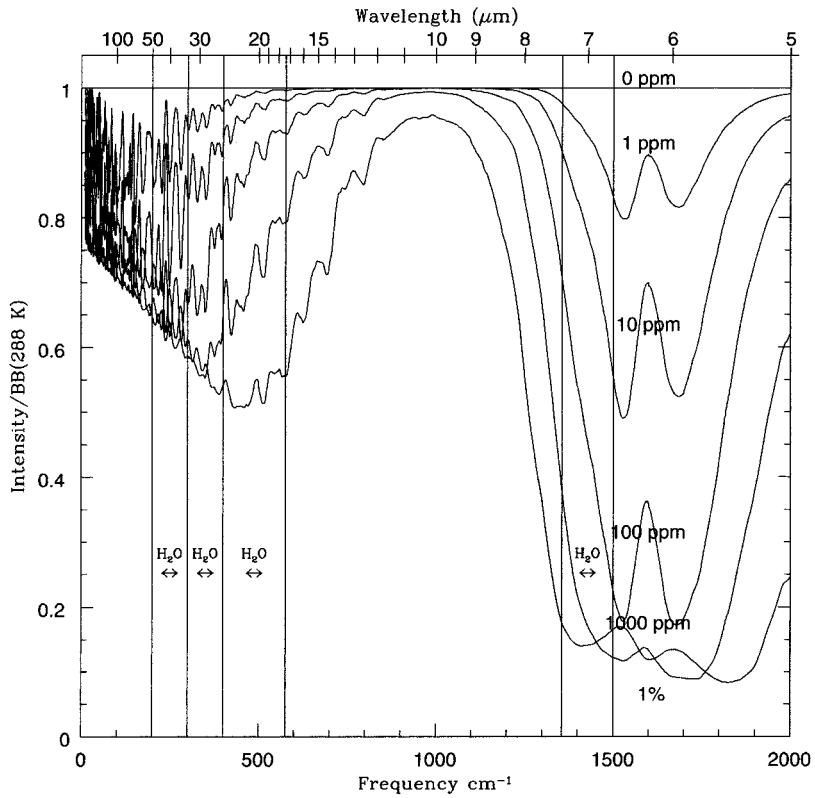

FIG. 6. The thermal emission spectrum of water is shown for six humidity levels ranging from completely dry to essentially saturated. In each case the Earth's water vapor vertical mixing ratio profile is used, but scaled to give the surface mixing ratios indicated. Dominant features are the 15–100 μm rotational bands and the 6 μm vibrational bands. Here and in subsequent figures, potential broad detection wavelength regions are indicated, chosen for their likelihood of producing a relatively clean detection of each species for an extrasolar terrestrial planet. BB, blackbody.

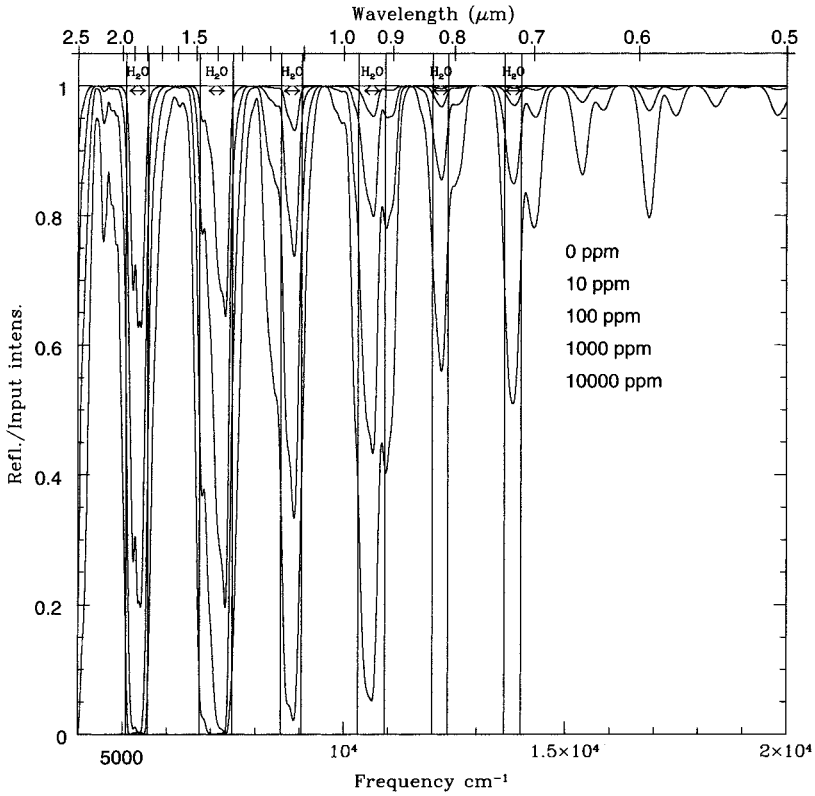

FIG. 7. The reflection spectrum of water is shown for five humidity levels, similar to Fig. 6. Dominant features are at 0.7, 0.8, and 0.9 μm in the visible and 1.1, 1.4, and 1.9 μm in the near-IR.

abundances is caused by the Earth's stratospheric temperature inversion (which is in turn caused by absorption of solar UV light by O_2 and O_3, and conversion to heat). Weaker bands show up at 9–11 μm when the CO_2 abundance climbs to ~1%. Measurements of even higher abundances of CO_2, ~10%, may be possible, and these will encroach further into the 8–13 μm window.

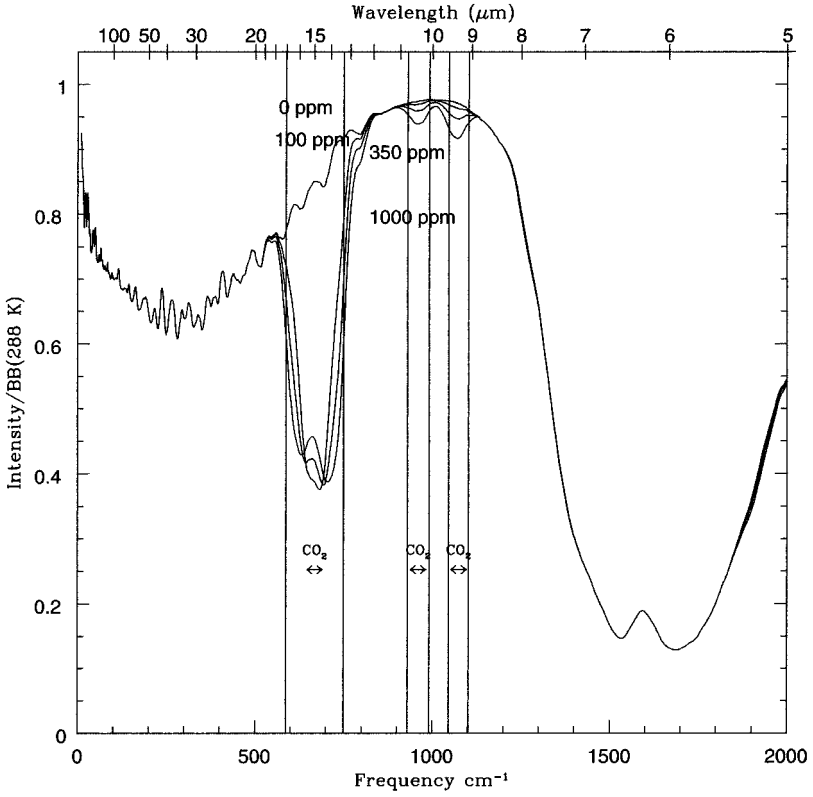

FIG. 8. The thermal emission spectrum of carbon dioxide is shown for four abundance levels. A nominal level of water vapor is assumed to be simultaneously present. The 15 μm feature of CO_2 dominates the spectrum, but at high abundances the weak 9 and 10 μm bands also begin to show up. Note the inversion in the core of the 15 μm band at high abundances, due to increased opacity in the warm stratospheric layer. BB, blackbody.

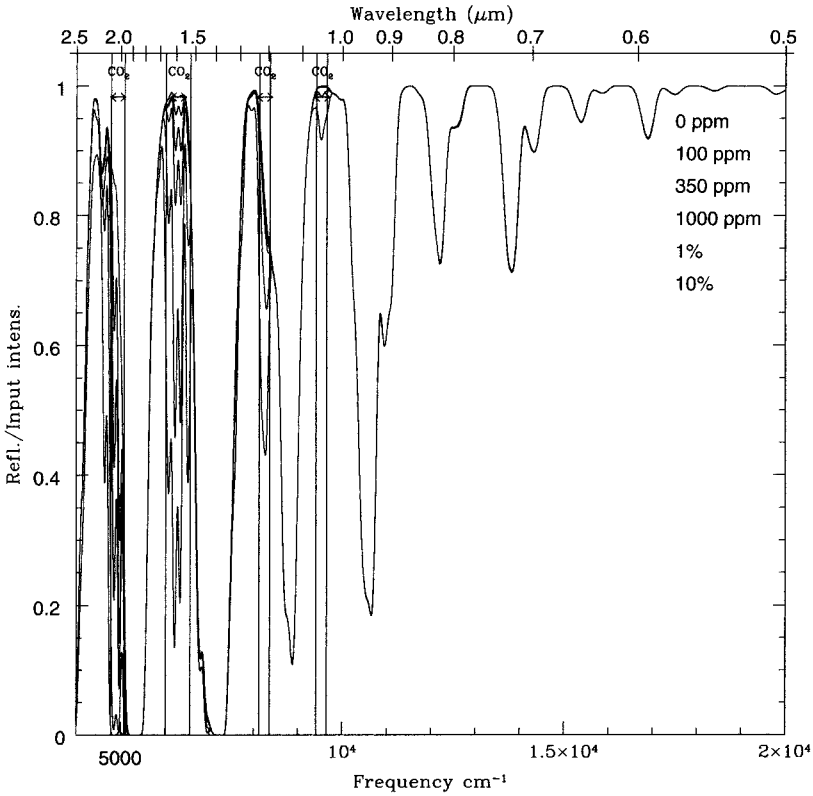

FIG. 9. The reflection spectrum of carbon dioxide is shown for six abundances. As in Figs. 8 and 10, a background abundance of water vapor is also included. At high abundances, CO_2 could be detected in the 1.06 and 1.3 μm bands, but to see lower abundances the 1.6 and 2.0 μm bands would be needed.

Visible-wavelength CO_2 features are shown in Fig. 9, superimposed on a background of H_2O absorption for the current average Earth abundance of water. The shortest wavelength feature of CO_2 is at 1.06 μm, and this will only become significant when the abundance is very high, on the order of 10%, which could well be the situation for an early-Earth atmosphere. The next shortest wavelength band is at 1.2 μm, in the wing of an H_2O band but nevertheless still appreciable at abundances of $\geq$1%, also an early-Earth indicator. The next available band of CO_2 is at 1.6 μm, located between H_2O bands. Here the strength is significant for abundances of CO_2 only about three times greater than present on Earth. Thus if the full range from 1.0 to 1.7 μm is available, this spectrum provides estimates across a wide range of CO_2 abundances.

Ozone (Figs. 10–12)

O_3 has a PAL of 6 ppm in the stratospheric "O_3 layer" around 25–35 km, with a lower abundance tail extending down to the surface. In the IR (Fig. 10) the main feature is at 9 μm, with a weaker band at 14 μm. However, if CO_2 is present in even small amounts the 14 μm feature will be mostly blocked. The 9 μm band is highly saturated and is essentially unchanged as the O_3 abundance varies from 1 to 6 ppm. This makes the 9 μm band a poor quantitative indicator of O_3, but what is likely much more important is that it is a highly sensitive indicator of the existence of even a trace amount of O_2. Silicate minerals and O_3 both have strong features in the 9 μm region, but there is little chance that the two could be confused because their spectral shapes are quite distinct. The closest match of a silicate feature to O_3 is that of the mineral illite, and even in that case the band shapes are readily distinguishable from that of O_3.

Visible-wavelength O_3 has a broad feature extending from ~0.5 to 0.10 μm, the so-called Chappuis bands, shown in Fig. 11. (A weak H_2O band falls in the middle of this broad O_3 feature, distorting its nominally triangular shape.) The abundance levels indicated in Fig. 11 represent the stratospheric O_3 layer, although the tropospheric abundance does contribute a small amount to the observed band. For quantitative analysis, the Chappuis bands might offer advantages because their absorption depths increase roughly linearly with abundance, and, in particular, they are not saturated at the present abundance level. The breadth of the Chappuis bands is at once an advantage, because only low resolution is needed

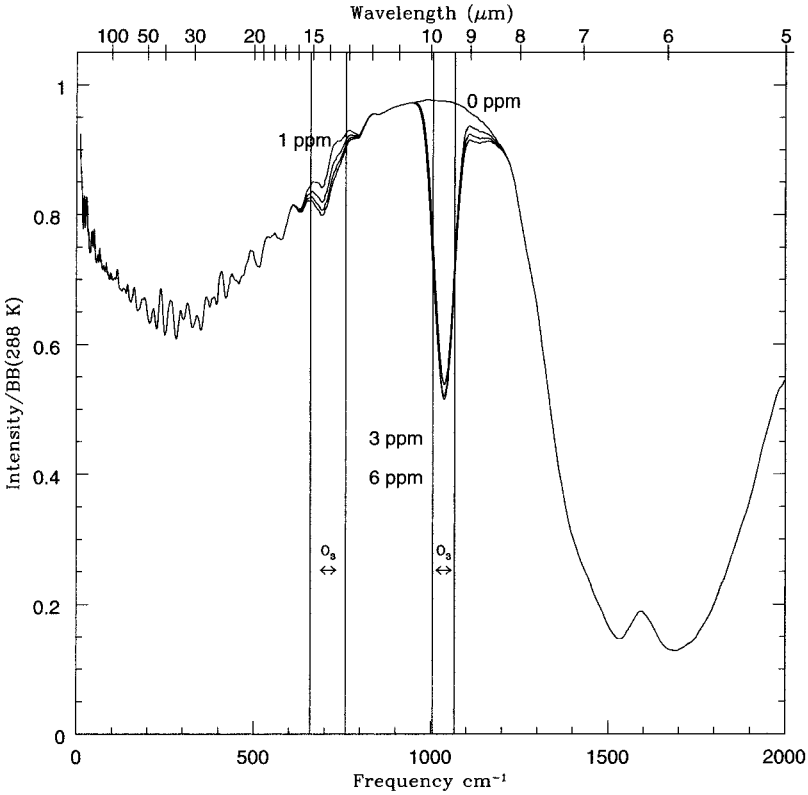

FIG. 10. The thermal emission spectrum of ozone is shown for four abundance levels, where the present Earth's mixing ratio profile, dominated by the stratospheric ozone layer, has been scaled, and the value indicated is that at the peak of the ozone layer. The 9 μm feature is saturated for all indicated abundances, and only the 14 μm feature, which would be hidden by any CO_2 present, is on the linear part of the curve of growth. BB, blackbody.

to detect them, and a disadvantage, because it is generally harder to distinguish broad features than narrow ones against a potentially complex or unknown background spectrum.

UV absorption by O_3 is very strong in the so-called Huggins bands (Fig. 12), which start to absorb at ~0.34 μm and increase dramatically toward 0.31 μm and shorter wavelengths. At

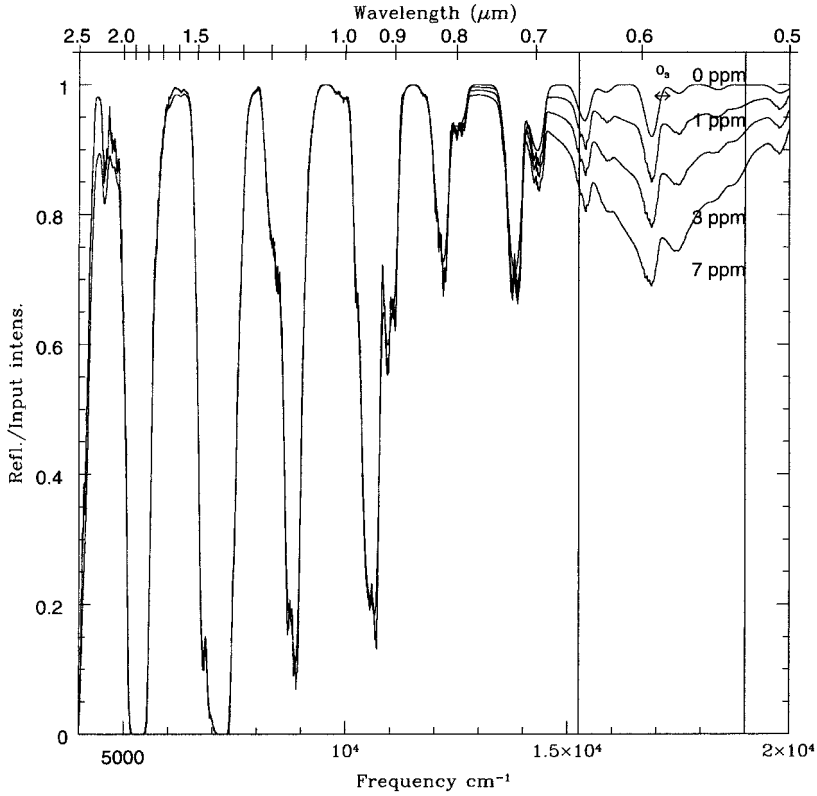

FIG. 11. The visible reflection spectrum of ozone is shown for four abundance levels, for conditions as given in the legend to Fig. 10. The broad 0.6 μm band intensity responds linearly to variations in mixing ratio.

PAL these bands are opaque from ~0.32 μm shortward and will be present for even very small amounts of O_3. Although there are perhaps more experimental difficulties working in the UV than at longer wavelengths, the extreme sensitivity of the Huggins bands makes this region an obvious potential target for a biosignature search.

Methane (Figs. 13 and 14)

CH_4 has a PAL of 1.6 ppm, uniformly mixed in the troposphere and decreasing in the stratosphere. In the mid-IR range (Fig. 13) the main CH_4 feature is at 7 μm wavelength, where it is overlapped by the 6 μm band of water and the adjacent bands of N_2O (both of which are in the background spectra in Fig. 13). The CH_4 feature nevertheless produces a weak absorption even at PAL; however, the combined effect of a falling Planck curve and the extra opacity contributed by water make this a possible but difficult observation. However, during its history, Earth's atmosphere has likely witnessed two types of high-CH_4 states: first, during the initial half of its life when the composition was more reducing than at present, and second, during later "CH_4 burst" conditions, where a 1% mixing ratio may have existed for limited periods of time (Bains *et al.*, 1999; Hesselbo *et al.*, 2000). In both cases the CH_4 band is strong enough to be seen in the wing of the water vapor band at 8–9 μm; therefore a detection may be possible.

In the visible to near-IR range, CH_4 (Fig. 14) has five relatively unobscured absorption features between 0.6 and 1.0 μm and two more at 1.7 and 2.4 μm wavelength. The features at 0.6, 0.7, 0.8, 0.9, and 1.0 μm have significant depth for high abundances, in the range 1,000 ppm to 1%, which is a range of great interest for the early Earth. The 1.7 and 2.4 μm features become significant at CH_4 levels of $\geq$100 ppm. Thus none of the visible features is useful at present abundance levels, but they could be very significant for $\geq$100 times PAL.

Nitrous oxide (Fig. 15)

N_2O is produced during microbial oxidation–reduction reactions, and nonbiological sources are apparently negligible. Thus it is a potential biosignature. It has a PAL of 310 ppb, uniformly mixed in the troposphere but disappearing in the stratosphere. In the mid-IR (Fig. 15), N_2O has a band near 8 μm, roughly comparable in strength to the adjacent CH_4 band but weak compared with the overlapping H_2O band. The background spectrum in Fig. 15 includes both

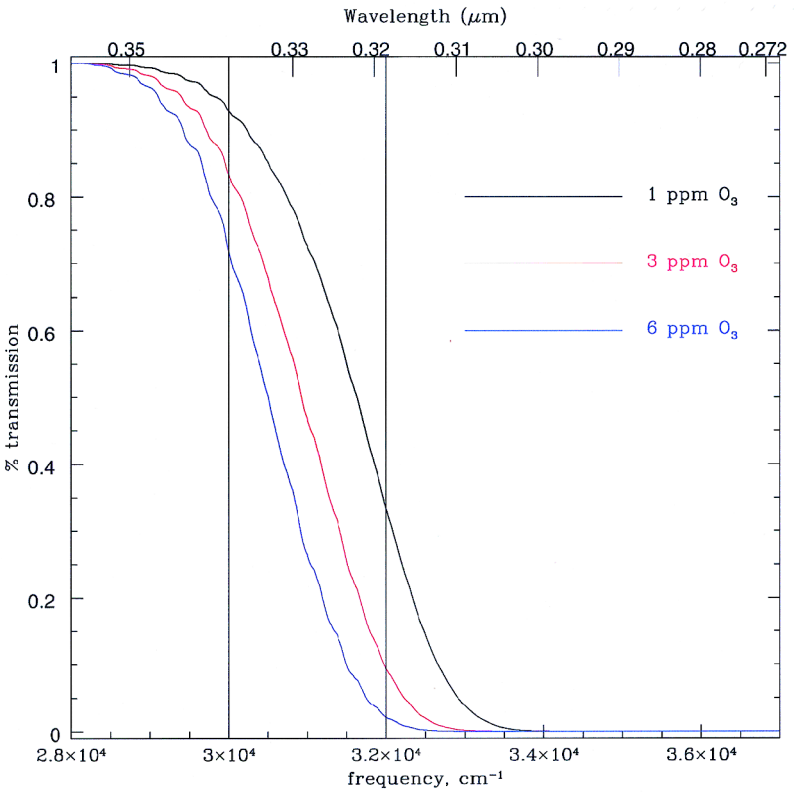

FIG. 12. The UV reflection spectrum of ozone is shown for three abundance levels in the stratospheric ozone layer, as discussed in the legends to Figs. 10 and 11. A wavelength band over which the intensity is roughly linear is indicated, around 0.33 μm. The core of the ozone band is at a yet shorter wavelength and is completely saturated, but could be used for ozone detection at much lower abundances, if no other absorption feature were present.

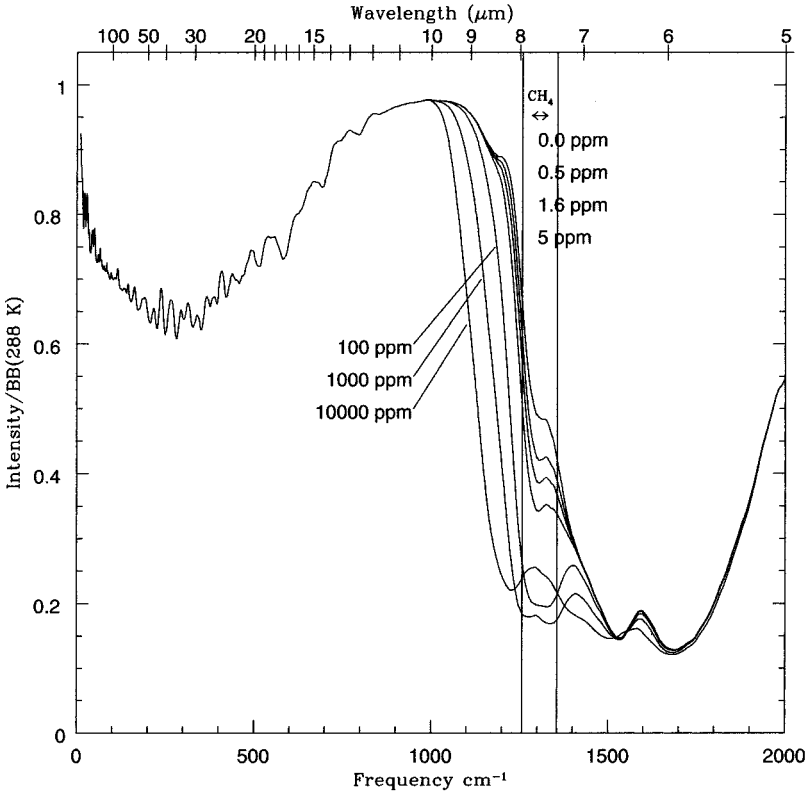

FIG. 13. The thermal emission spectrum of methane is shown for seven mixing ratios. The 7 μm band would show up more distinctly if it were not for the presence of water in the background, which in this case is a serious potential spectral contaminant. Present terrestrial methane levels will only produce a weak feature on the side of the dominant water band, but high methane levels, such as may have been present in the early Earth's atmosphere, could produce a stronger, more easily detectable feature. BB, blackbody.

H_2O and CH_4. Fortunately, the absorption patterns of these three species are different, so in principle their contributions may be separable. Spectral features of N_2O will become progressively more apparent in atmospheres having less H_2O vapor. An additional band at 17 μm may well be totally obscured by CO_2; therefore it should not be expected to be useful. There are no significant N_2O features in the visible range. Atmospheric concentrations of N_2O will decrease with decreasing O_2 concentrations if the biological source strength remains constant (Kasting and Donahue, 1980).

Oxygen (Fig. 16)

Oxygen has a PAL of 21%, uniformly mixed. In the visible (Fig. 16) there are three potentially significant features: at 0.69 (Fraunhofer B band), 0.76 (Fraunhofer A band), and 1.26 μm. Among these, the 0.76 μm feature is the strongest one, having appreciable depth at an abundance level of $\geq$1%, making it potentially very useful as a biosignature. All three bands are essentially unobscured in the present Earth spectrum.

In the IR there are no significant O_2 features. In the submillimeter region there are strong O_2 lines; however, these wavelengths are much longer than those considered here.

Summary: band lists and curves of growth (Tables 1 and 2)

The spectral bands discussed above are listed in Table 1, starting with the IR bands within the 7 and 50 μm range (including the two continuum windows that are useful for temperature measurement). The visible bands between 0.3 and 2.5 μm are then listed (of which most lie between 0.3 and 1.1 μm). The table columns give the species name, the wavenumbers of the bands (minimum, maximum, and average), the spectral resolution [average/(maximum − minimum)], and the corresponding wavelength values. The wavenumber entries were determined graphically by visual inspection of the figures and thus are a function of both each species itself as well as any encroachment by neighboring spectral features. The values of full width at half-maximum (FWHM) intensity, and also spectral resolutions, are intended to represent approximately optimum detection bandwidths, in the sense of a matched filter, based on the assumption that the spectra will be determined by only the species considered here. Therefore if significantly different spectra are anticipated, then higher spectral resolutions might be needed in order to permit unambiguous feature identifications.

The average depth of molecular absorption is

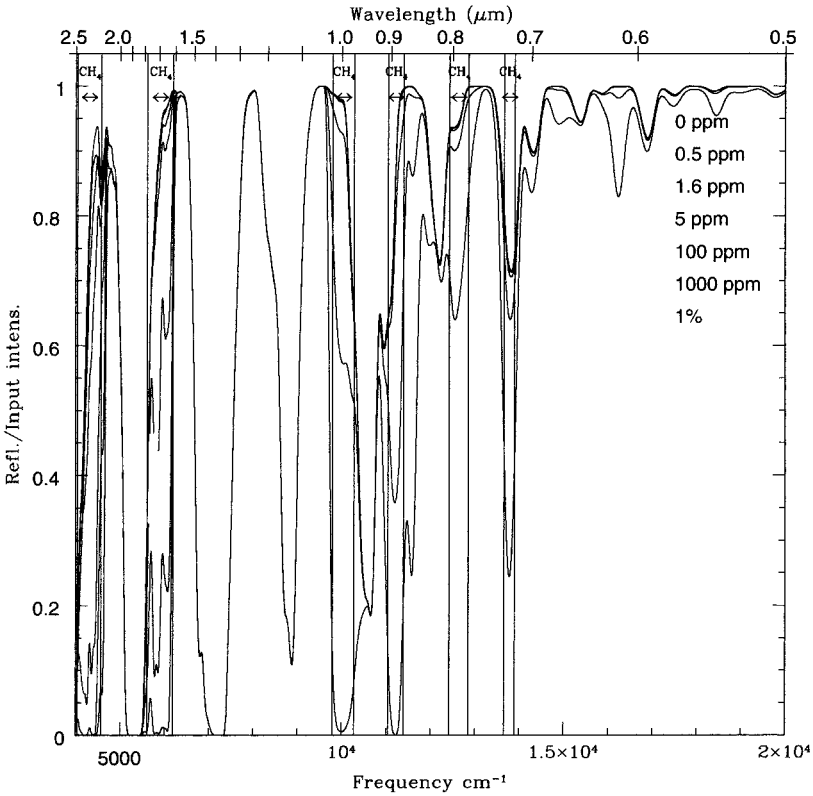

FIG. 14. The visible reflection spectrum of methane is shown for seven abundance levels. At low abundances, methane would be detectable only at the longest wavelength, around 2.4 μm. However, at moderate and high abundances methane could be detected in the 0.7, 0.8, 0.9, and 1.0 μm bands.

listed in Table 2, as a function of mixing ratio, for the present Earth (i.e., present base pressure and temperature profile) from a curve of growth analysis (Goody and Yung, 1989). Each depth is calculated from the continuum levels indicated in the figures, i.e., for H_2O, the depth is measured from a flat featureless continuum, and for all other species the depth is measured with respect

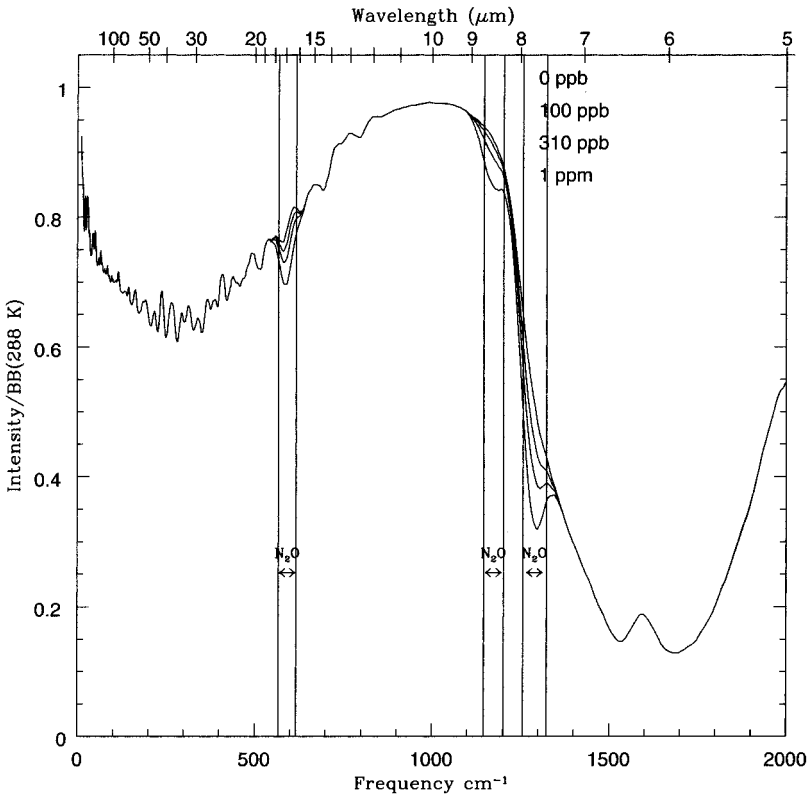

FIG. 15. The thermal emission spectrum of nitrous oxide is shown for four abundance levels. As with methane, nitrous oxide only becomes detectable in the 8 μm region at high abundances, and it will be partially blended with methane as well as the dominant water feature. (There is no corresponding visible wavelength feature of nitrous oxide.) BB, blackbody.

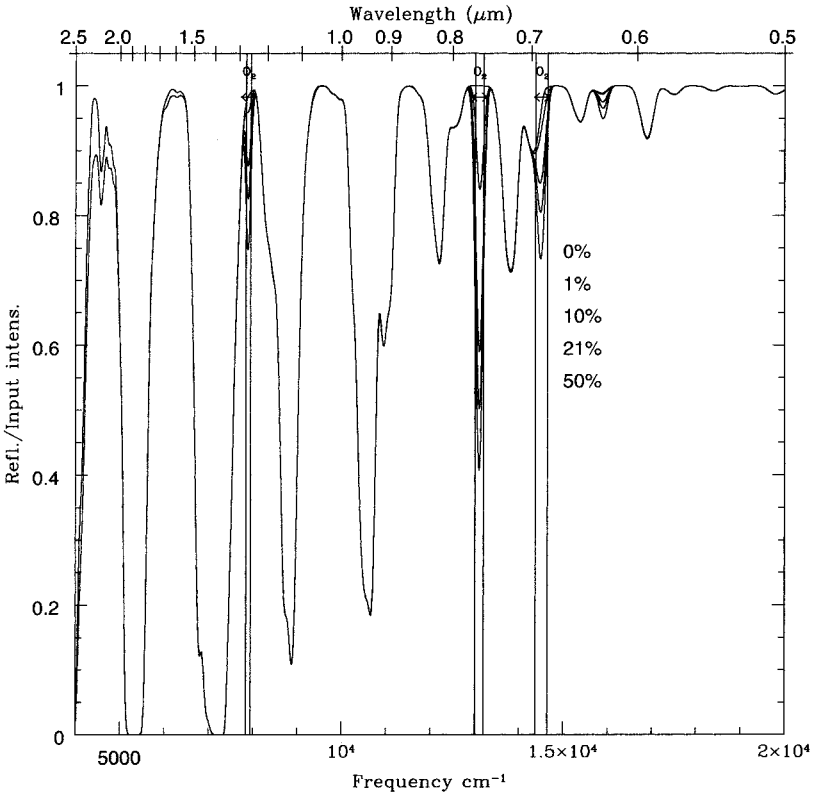

FIG. 16. The visible reflection spectrum of molecular oxygen is shown for five abundance levels. Candidate detection bands are the 0.7 and 0.76 μm bands, which are spectrally relatively narrow, but which are roughly linear in their response to oxygen abundance. At 0.76 μm there is no known interfering feature. (There is no corresponding feature for oxygen in the mid-IR wavelength range.)

to the nominal water continuum indicated in the figures. Thus the depth values include an element of realism in the context of planet detection (concerning the presence of water, at least) that would not be present if the calculations were all done with respect to a featureless background. For each spectral band the integration is done between the nominal FWHM limits drawn in each figure and listed in Table 1. Thus the absorbed area could also be written as the product of FWHM and depth. For example, the average depth of the O_2 Fraunhofer A band at 13,105 cm^{-1} is 0.47 at PAL and in a cloud-free atmosphere.

These tables can be used to create model spectra for spectral resolutions at, or cruder than, that assumed here, and hence serve as a useful simulation database for different TPF/Darwin configurations.

SPECTRAL FEATURES FROM THE PLANET'S SURFACE

A planet's spectrum should vary due to seasonal changes, weather, and different surface types rotating in and out of view. On a timescale longer than that of a rotational period or typical change in weather, these effects should average out and not present any serious complications to detecting atmospheric biosignature spectral signatures. However, there are potential benefits associated with observing variations over time. For example, it may be possible to derive the planet's rotational period, existence of weather (time-varying water clouds are indicative of water oceans), surface biosignatures, existence of water oceans, and perhaps even ocean or ice fraction. One might expect that the differing albedos and surface temperatures from different parts of an unresolved Earth-like planet will cancel each other. This in fact does not occur, mostly because of nonuniform illumination and viewing angle, and, in fact, a relatively small part of the visible hemisphere dominates the total flux from a spatially unresolved planet. Because of this, there is the potential to detect surface features from TPF/Darwin data.

Flux variations in the optical wavelength range that occur on a rotational timescale and that are caused by different types of surfaces rotating in and out of view (e.g., oceans, including specular reflection, land, and ice cover) can be as high as 150–200% for a cloud-free Earth. Flux variations can be as high as 650% for an ice-covered planet with ice-free liquid oceans. These numbers are re-

Table 1. Molecular Species and Spectral Bands Used in this Study

		σ (cm^{-1})				λ (μm)		
Band	*Species*	*Minimum*	*Maximum*	*Average*	*Resolution*	*Minimum*	*Maximum*	*Average*
1	H_2O	200	300	250	2	33.33	50.00	40.00
2	H_2O	300	400	350	4	25	33.33	28.57
3	H_2O	400	576	488	3	17.36	25	20.49
4	H_2O	1,356	1,500	1,428	10	6.67	7.37	7.00
5	CO_2	587	750	668	4	13.33	17.04	14.96
6	CO_2	930	990	960	16	10.75	10.10	10.42
7	CO_2	1,046	1,102	1,074	19	9.56	9.07	9.31
8	O_3	1,005	1,067	1,036	17	9.37	9.95	9.65
9	CH_4	1,257	1,356	1,306	13	7.37	7.96	7.65
10	CH_4	1,150	1,356	1,253	6	7.37	8.70	7.98
11	Cont.	804	986	895	5	10.14	12.44	11.17
12	Cont.	1,082	1,226	1,154	8	8.16	9.24	8.67
13	H_2O	5,080	5,580	5,330	11	1.79	1.97	1.88
14	H_2O	6,740	7,480	7,110	10	1.34	1.48	1.41
15	H_2O	8,580	9,050	8,815	19	1.10	1.17	1.13
16	H_2O	10,320	10,930	10,625	17	0.91	0.97	0.94
17	H_2O	12,000	12,350	12,175	35	0.81	0.83	0.82
18	H_2O	13,630	14,000	13,815	37	0.71	0.73	0.72
19	CO_2	4,780	5,080	4,930	16	1.97	2.09	2.03
20	CO_2	6,020	6,570	6,295	11	1.52	1.66	1.59
21	CO_2	8,120	8,360	8,240	34	1.20	1.23	1.21
22	CO_2	9,410	9,650	9,530	40	1.04	1.06	1.05
23	O_2	7,840	7,950	7,895	72	1.26	1.28	1.27
24	O_2	13,010	13,200	13,105	69	0.76	0.77	0.76
25	O_2	14,380	14,650	14,515	54	0.68	0.70	0.69
26	O_3	15,250	19,000	17,125	5	0.53	0.66	0.58
27	O_3	30,000	32,000	31,000	16	0.31	0.33	0.32
28	CH_4	4,040	4,570	4,305	8	2.19	2.48	2.32
29	CH_4	5,610	6,190	5,900	10	1.62	1.78	1.69
30	CH_4	9,790	10,280	10,035	20	0.97	1.02	1.00
31	CH_4	11,040	11,390	11,215	32	0.88	0.91	0.89
32	CH_4	12,420	12,850	12,635	29	0.78	0.81	0.79
33	CH_4	13,660	13,900	13,780	57	0.72	0.73	0.73

Two IR continuum (Cont.) bands (11 and 12) are also given, where in a cloud-free atmosphere, emission from the surface might be seen. Columns 3–5 give the nominally optimum wavenumber values (minimum, maximum, and average) for each band. Column 6 gives the corresponding spectral resolution. Columns 7–9 give the same information in terms of wavelength.

duced to 10–20% in the case of Earth-like cloud cover (Ford *et al.*, 2001). This variation is a direct consequence of the large differences in albedo among ocean, land, and ice (<10% for ocean, >30–40% for land, >60% for snow and some types of ice). Discriminating among these different surfaces need not require a specific spectral signature; therefore the required observation time could be shorter than that for detecting spectral features.

It may be possible to detect surface biosignatures if they make up a large fraction of a planet's surface (e.g., Schneider *et al.*, 2000). An interesting example from the Earth is the "red edge" signature from photosynthetic plants at ~750 nm where the reflectivity changes by almost an order of magnitude (Ford *et al.*, 2001). This is much greater than the reflectivity change on either side of green wavelengths (less than a factor of 2) due to chlorophyll absorption. Photosynthetic plants have developed this strong IR reflection as a cooling mechanism to prevent overheating, which in turn would cause chlorophyll to degrade. A simple calculation for the integrated reflectivity difference between a vegetation-free Earth and our own Earth (assuming that one-third of the Earth is covered with land and that one-third of the land is covered with vegetation) gives 2%. Considering geometry, time resolution on a rotational timescale, and directional scattering effects, this number should be considerably larger when a large forested area is in view. A detailed calcula-

Table 2. Curve-of-Growth Values for Each Molecular Band Are Listed Here, First for the Thermal Emission IR Region, and Second for the Visible, Near-IR, and UV Regions

Thermal

Gas, concentration	*Curve-of-growth value at given wavenumber*			
H_2O	250 cm^{-1}	350 cm^{-1}	488 cm^{-1}	1,428 cm^{-1}
1 ppm	0.090	0.043	0.072	0.048
10 ppm	0.213	0.124	0.025	0.161
100 ppm	0.341	0.279	0.068	0.427
1,000 ppm	0.377	0.416	0.153	0.747
10,000 ppm	0.339	0.436	0.226	0.850
CO_2	668 cm^{-1}	960 cm^{-1}	1,074 cm^{-1}	
100 ppm	0.470	0.029	0.037	
350 ppm	0.520	0.037	0.050	
1,000 ppm	0.548	0.054	0.075	
10,000 ppm	0.549	0.153	0.207	
O_3	1,036 cm^{-1}	710 cm^{-1}		
1 ppm	0.382	0.141		
3 ppm	0.406	0.154		
6 ppm	0.405	0.162		
N_2O	592 cm^{-1}	1,174 cm^{-1}	1,290 cm^{-1}	
100 ppb	0.014	0.008	0.050	
310 ppb	0.031	0.023	0.095	
1,000 ppb	0.063	0.063	0.160	
CH_4	1,306 cm^{-1}			
0.5 ppm	0.056			
1.6 ppm	0.091			
5.0 ppm	0.137			
100 ppm	0.300			
1,000 ppm	0.330			
10,000 ppm	0.262			

Visible/near-IR/UV

Gas, concentration	*Curve-of-growth value at given wavenumber*					
H_2O	5,330 cm^{-1}	7,110 cm^{-1}	8,815 cm^{-1}	10,625 cm^{-1}	12,175 cm^{-1}	13,815 cm^{-1}
10 ppm	0.236	0.178	0.041	0.025	0.003	0.003
100 ppm	0.586	0.485	0.172	0.124	0.025	0.024
1,000 ppm	0.901	0.830	0.500	0.401	0.118	0.130
10,000 ppm	0.990	0.988	0.885	0.795	0.379	0.441
CO_2	4,930 cm^{-1}	6,295 cm^{-1}	8,240 cm^{-1}	9,530 cm^{-1}		
100 ppm	0.170	0.007	0.005	0.0002		
350 ppm	0.309	0.030	0.012	0.0006		
1,000 ppm	0.443	0.065	0.027	0.001		
1%	0.667	0.260	0.116	0.011		
10%	0.714	0.566	0.331	0.062		
CH_4	4,305 cm^{-1}	5,900 cm^{-1}	10,035 cm^{-1}	11,215 cm^{-1}	12,635 cm^{-1}	13,780 cm^{-1}
0.5 ppm	0.005	0.003	0.063	0.001	0.0009	0.002
1.6 ppm	0.009	0.012	0.011	0.002	0.0009	0.002
5.0 ppm	0.111	0.039	0.025	0.004	0.0009	0.003
100 ppm	0.462	0.298	0.039	0.060	0.010	0.010
1,000 ppm	0.587	0.630	0.315	0.417	0.032	0.073
10,000 ppm	0.627	0.814	0.881	0.818	0.267	0.455
O_2	7,895 cm^{-1}	13,105 cm^{-1}	14,515 cm^{-1}			
1%	0.023	0.150	0.025			
10%	0.104	0.388	0.088			
21%	0.153	0.474	0.124			
50%	0.230	0.565	0.181			
O_3	17,125 cm^{-1}	31,000 cm^{-1}				
1 ppm	0.048	0.305				
3 ppm	0.112	0.531				
7 ppm	0.195	0.692				

For each species and abundance level, the average depth of each important spectral feature is listed, with the central wavenumber of the corresponding band noted at the top of each column. Refer to Table 1 for bandwidths and corresponding wavelength values. Entries range from weak lines (e.g., 0.029, or 2.9% average depth) to strong lines (e.g., 0.474, or 47.4% average depth). The values given are appropriate for an Earth-like temperature structure and mixing ratio profile for each species. For O_3 the mixing ratio values refer to the peak abundance in the stratosphere.

tion is needed. We note that this vegetation signature has been detected by the Galileo spacecraft from a small part of the Earth (Sagan *et al*., 1993) and has since been used by Earth-oriented operational satellites on a regular basis. Some photosynthetic marine life also has a wavelength-dependent signature similar to land vegetation. In addition, phytoplankton blooms can cause a temporal change in large areas of the ocean. The ocean is very dark in the optical and has strong water absorption bands in the IR, however, and so most of the reflected flux from the Earth does not come from the ocean even though it is a large fraction of the surface area. This means it will be difficult to detect the color difference due to spatial or temporal variability of photosynthetic marine organisms.

Recently Woolf *et al*. (2002) and Arnold *et al*. (2002) have tentatively detected the chlorophyll red edge in an integrated-Earth spectrum, obtained by observing sunlight reflected from the Earth to the dark side of the moon and back to Earth, the so-called Earthshine spectrum. This same observation highlights the strong Rayleigh scattered continuum, prominent in the 0.3–0.5 μm region, a potential planet-characterization signal, which, along with the chlorophyll feature, deserves further study.

For a planet with nonzero obliquity, the seasonal flux variation might also be detectable. Total seasonal change for our Earth's global albedo is smaller than the expected rotational variation [~7% from simulations of Earthshine by Goode *et al*. (2001)], but this could be much different for planets with different obliquities or with different orbital inclinations. Rotational variation in the mid-IR flux could also be detected, but for the Earth is expected to be lower than the optical flux variation because the surface temperature does not vary as much as the surface albedo across the Earth. In the mid-IR the seasonal variation could be larger than the mid-IR rotational variation because of seasonal temperature changes. Planets having uniform cloud cover such as Venus would show no rotational or seasonal change in the spatially unresolved flux.

Summary

A TPF/Darwin architecture that is capable of detecting spectral features at high signal/noise ratios will also be able to detect 10% changes in the flux. The opportunity to derive physical properties of the planet on a rotational or seasonal timescale from the TPF/Darwin data is an important addition to the main goal of TPF/Darwin to detect and characterize Earth-like planets. There is a large parameter space of possible physical characteristics of Earth-like extrasolar planets, and a more careful study of time variation and surface features is recommended.

CONCLUSIONS: WAVELENGTH RANGES AND PRIORITIZATION OF SPECTRAL FEATURES

Wavelength range

Here we use the data in IR and Visible Molecular Band Features to assess the minimal wavelength coverage required from TPF/Darwin in order to characterize terrestrial planets as Earth-like and possibly life-bearing.

In the thermal IR, it is absolutely essential to observe the 15 μm CO_2 band and the 9.6 μm O_3 band. O_3 is our best biosignature gas in the mid-IR range. One should also observe the entire 8–12 μm "window" region because that offers the best chance for estimating the planet's surface temperature. Some measure of H_2O is required, which can be obtained from either the 6.3 μm band or the rotation band that extends from 12 μm out into the microwave region. Finally, it would be helpful to observe the 7.7 μm band of CH_4 because this is potentially a good biosignature gas for early-Earth–type planets. Thus, the minimum wavelength coverage would be 8.5–20 μm, and optimal coverage should extend from 7 to 25 μm.

In the visible/near-IR, it is essential to observe the 0.76 μm band of O_2. The broadband 0.45–0.75 μm O_3 absorption will need about the same signal/noise value and, on a cloud-covered planet or one with a lower oxygen abundance, may well be easier to detect. One also needs at least one strong H_2O band—we suggest 0.94 μm, which we can obtain by going out to 1.0 μm. CO_2 is much more difficult to observe in the visible/near-IR. If the planet is CO_2-rich, the best feature is at 1.06 μm, which would require wavelength coverage out to at least 1.1 μm. This should not be a principal determinant of the wavelength range to be observed, though, because this band is weak, even in the spectrum of Venus. For terrestrial gas abundances, the shortest wavelength bands that show well are at 2.00 and 2.06 μm. Finally, the best CH_4 band shortward of 1.0 μm is at 0.88 μm,

though it only shows at considerably greater abundance than terrestrial. Required wavelength coverage would be 0.7–1.0 μm, and we would prefer to see $\sim$0.5 μm (to look for broadband absorption by O_3) to $\sim$1.1 μm (to detect CO_2).

O_3 might be detected in UV range (at 0.34–0.31 μm); however, more studies are required to evaluate potential interferences. On Earth, only O_2 and NO_2 absorb significantly in the O_3 region, but on other planets, there might be competing sources of opacity.

Prioritization

Deciding which features in each wavelength regimen are most important to observe is not a simple task, and in the spectroscopic community as a whole, considerable diversity of choice might be advocated. However, the present group of authors agrees on the following:

1. Detection of O_2 or its photolytic product O_3 is our highest priority because O_2 is our most reliable biosignature gas. Possible "false-positives" for O_2 have been identified (Kasting, 1997; Léger *et al.*, 1999). One such pathological case involves the abiotic production of O_2 from H_2O photolysis followed by rapid hydrogen escape from a runaway greenhouse atmosphere. Another such case involves buildup of O_2 from the same abiotic process on a frozen planet somewhat larger than Mars (0.1–0.2 times Earth mass). The frozen surface would keep O_2 from reacting with reduced minerals in the crust, while the mass range would preclude nonthermal escape of O atoms without creating enough internal heat to sustain volcanic outgassing of reduced gases. Both of these cases could presumably be identified spectroscopically. For a "normal" Earth-like planet situated within the habitable zone, free O_2 is a reliable indicator of life.
2. O_3 is as reliable a bioindicator as O_2. However, it provides somewhat different information. Because of its nonlinear dependence on O_2 abundance, O_3 is easier to detect at low O_2 concentrations. However, it is a relatively poor indicator of how much O_2 is actually present. It is difficult to say which type of information is more useful. A positive identification of either gas would be very exciting and significant.
3. Another category of important observable features includes water vapor and the 8–12 μm continuum. H_2O is not a bioindicator; however, its presence in liquid form on a planet's surface is considered essential to life. Unfortunately, observations that show gaseous water vapor alone do not sufficiently constrain the conditions to determine whether the atmosphere is near saturation. Observation of the 8–12 μm continuum could, in some cases (such as present-day Earth), allow us to determine a planet's surface temperature, which is also an important constraint on life. However, the atmospheres of planets that are more than $\sim$20K warmer than Earth (i.e., >310K) will be opaque in this region because of continuum absorption by water vapor. Such planets are also susceptible to a runaway or "moist" greenhouse effect (Kasting, 1988), so the range of conditions where this occurs and the planet is also habitable will likely be limited. Planets with 1-bar atmospheres and surfaces warmer than $\sim$340K would lose their water relatively quickly (Kasting, 1988). Cloud cover (as on Venus) could also obscure the surface and preclude the determination of temperature. Indeed, it would be difficult or impossible for observations to distinguish a planet like Venus (with a cold cloud layer) from a planet with a cold, ice-covered surface. Thus, although there is an argument in favor of observing in the mid-IR range, it is balanced by the availability in the visible range of both O_2 and O_3 features.
4. The carbon-containing gases CO_2 and CH_4 can each provide useful information. In the mid-IR range, CO_2 is the easiest of all species to observe. CO_2 is required for photosynthesis and for other important metabolic pathways. Furthermore, it provides good evidence that we are dealing with a terrestrial planet. It is hard to imagine how a moist, rocky planet from which hydrogen can escape could *not* have CO_2 in its atmosphere. Even if carbon were outgassed in a more reduced form, some fraction of it ought to be oxidized to CO_2 by reaction with oxygen formerly in water.
The presence of CH_4 would provide interesting, but ambiguous, information. According to at least some models of atmospheric evolution (e.g., Kasting and Brown, 1998), CH_4 is expected to have been present at mixing ratios of $\sim 10^{-3}$ in the Late Archean atmosphere (2.5–3.0 billion years ago). The high concentrations of CH_4 at this time would have indi-

cated production by methanogenic bacteria. But, CH_4 could have been produced abiotically as well. About 1% of the carbon released from midocean ridge volcanism today is in the form of CH_4 (the rest is CO_2). If the early mantle was more reduced, most of the carbon released from submarine outgassing could have been in the form of CH_4, and abiotic CH_4 mixing ratios could have exceeded 10^{-4} (Kasting and Brown, 1998). So, we would probably require additional information to decide whether a CH_4-rich atmosphere was really an indication of life.

5. Determining the size of the planet is an important component of our understanding of habitability. By equating color temperature for selected spectral regions with physical temperature and using the observed flux, we can use Planck's Law to obtain the surface area of the planet. We can use the observed Solar System relationship among mass, radius, and thermal environment to infer the likely planet mass, and to consider whether this is or is not likely to be a planet with current or past operative geological activity. Geological activity is important for maintaining chemical resources for life as well as habitable conditions at the surface of the planet (Lunine, 1999a). It might be possible in the future to estimate planet size from visible to near-IR radiation by using observations of photometric mass or color mass.

CODA: SOME CAUTIONARY TALES FROM RECENT HISTORY

The challenge of interpreting observations of terrestrial planets in terms of their basic characteristics is not terribly different from that faced in the detection and characterization of other astronomical objects. Three tales provide both encouragement and caution in this regard. Debate raged for decades over whether the "spiral nebulae" were large and distant collections of stars, or nearby agglomerations of gas. The issue was finally settled in the 1920s when larger telescopes were able to resolve the nebulae into large assemblages of stars (Hubble, 1926). Thus, high spatial resolution won out over spectroscopy, but one can speculate that advances in spectroscopic understanding of stars and in the technology of spectrometers would have revealed the essential feature of galaxies as being composed of stars.

Spectra and images of Mars improved throughout the 20th Century, and yet it required close-up spacecraft observations to reveal the true nature of the Red Planet. Misinterpretation of spectroscopic data, including gross overestimates of the CO_2 partial pressure, and seasonal changes in surface color and brightness were interpreted as vegetation changes when in fact they were caused by the movement of dust globally (Glasstone, 1968). While Earth-based Hubble images have been spectacularly successful in providing sharp images of Mars, even these would have been unable to reveal the valley networks and other surface features indicative of a Martian surface much wetter in the past than at present (Zahnle, 2001). Finally, 35 years of spectroscopy of Saturn's moon Titan, ranging from the optical to the millimeter part of the spectrum, revealed the presence of an atmosphere and a number of interesting hydrocarbon species (as well as carbon monoxide). However, the basic nature of the atmosphere—whether tenuous and predominantly methane or dense and predominantly a spectroscopically inactive gas—could not be resolved from Earth. It required the close flyby of Voyager 1, and multiple remote sensing techniques on the spacecraft, to reveal an atmosphere of nitrogen four times denser at Titan's surface than is Earth's nitrogen atmosphere at sea level. And, despite the capabilities of the Hubble telescope and ground-based adaptive optics imaging, the surface of Titan remains poorly understood (Lunine, 1999b).

These lessons from extragalactic and Solar System astronomy should not discourage attempts to characterize extrasolar terrestrial-sized bodies, but they emphasize the need to apply as broad a range of sensing capabilities as possible. This is consistent with our conclusion that both optical spectroscopy and IR spectroscopy are important, if not required, to characterize fully Earths around other stars. And, we should be prepared for debates about the nature of discovered planets that will last for decades, debates that may not be resolved until techniques of hitherto unimagined power are fielded in the heavens in the distant future.

ABBREVIATIONS

FWHM, full width at half-maximum; PAL, present atmospheric level; SAO, Smithsonian Astro-

physical Observatory; TPF, Terrestrial Planet Finder.

REFERENCES

Arnold, L., Gillet, S., Lardière, O., Riaud, P., and Schneider, J. (2002) A test for the search for life on extrasolar planets: looking for the terrestrial vegetation signature in the Earthshine spectrum. *Astron. Astrophys.* (in press).

Bains, S., Corfield, R.M., and Norris, R.D. (1999) Mechanisms of climate warming at the end of the Paleocene. *Science* 285, 724–727.

Beichman, C.A., Woolf, N.J., and Lindensmith, C.A. (1999) *The Terrestrial Planet Finder: A NASA Origins Program to Search for Habitable Planets*, JPL Publication 99-3, Jet Propulsion Laboratory, Pasadena, CA.

Caroff, L.I. and Des Marais, D.J. (2000) Pale Blue Dot 2 Workshop: habitable and inhabited worlds beyond our Solar System. In *Pale Blue Dot 2 Workshop*, edited by L.I. Caroff and D.J. Des Marais, NASA/CP, NASA Ames Research Center, Moffett Field, CA, p. 320.

Cruikshank, D.P. (1983) The development of studies of Venus. In *Venus*, edited by D.M. Hunten, L. Colin, T.M. Donahue, and V.I. Moroz, University of Arizona Press, Tucson, pp. 1–9.

Committee on the Origin and Evolution of Life (2002) *Signs of Life: A Workshop on Life Detection*, National Academy Press, Washington, DC.

DeDuve, C. (1995) *Vital Dust*, BasicBooks, New York.

Des Marais, D.J., ed. (1997) *The Blue Dot Workshop: Spectroscopic Search for Life on Extrasolar Planets*, NASA Conference Publication 10154, NASA Ames Research Center, Moffett Field, CA.

Des Marais, D.J. and Walter, M.R. (1999) Astrobiology: exploring the origins, evolution and distribution of life in the universe. *Annu. Rev. Ecol. Systematics* 30, 397–420.

Des Marais, D.J., Harwit, M., Jucks, K., Kasting, J., Lin, D., Lunine, J., Schneider, J., Seager, S., Traub, W., and Woolf, N. (2001) *Biosignatures and Planetary Properties to be Investigated by the TPF Mission*, JPL Publication 01-008, Jet Propulsion Laboratory, Pasadena, CA, p. 48.

Ford, E.B., Seager, S., and Turner, E.L. (2001) Characterization of extrasolar terrestrial planets from diurnal photometric variability. *Nature* 412, 885–887.

Glasstone, S. (1968) *The Book of Mars*, NASA, Washington, DC.

Goode, P.R., Qui, J., Yurchyshyn, V., Hickey, J., Chu, M.-C., Kolbe, E., Brown, C.T., and Koonin, S.E. (2001) Earthshine observations of the Earth's reflectance. *Geophys. Res. Lett.* 28, 1671–1674.

Goody, R.M. and Yung, Y.L. (1989) *Atmospheric Radiation: Theoretical Basis*, Oxford University Press, New York.

Gould, S.J. (1996) *Full House*, Three Rivers Press, New York.

Hesselbo, S.P., Grocke, D.R., Jenkyns, H.C., Bjerrum, C.J., Farrimond, P., Morgans Bell, H.S., and Green, O.R. (2000) Massive dissociation of gas hydrate during a Jurassic oceanic anoxic event. *Nature* 406, 392–395.

Hoffman, P.F., Kaufman, A.J., Halverson, G.P., and Schrag, D.P. (1998) A Neoproterozoic snowball Earth. *Science* 281, 1342–1346.

Hubble, E.P. (1926) A spiral nebula as a stellar system: Messier 33. *Astrophys. J.* 63, 236–274.

Ingersoll, A.P. (1969) The runaway greenhouse: a history of water on Venus. *J. Atmos. Sci.* 26, 1191–1198.

Kasting, J.F. (1988) Runaway and moist greenhouse atmospheres and the evolution of Earth and Venus. *Icarus* 74, 472–494.

Kasting, J.F. (1997) Habitable zones around low mass stars and the search for extraterrestial life. *Orig. Life* 27, 291–307.

Kasting, J.F. and Brown, L.L. (1998) Setting the stage: the early atmosphere as a source of biogenic compounds. In *The Molecular Origins of Life: Assembling the Pieces of the Puzzle*, edited by A. Brack, Cambridge University Press, New York, pp. 35–56.

Kasting, J.F. and Donahue, T.M. (1980) The evolution of atmospheric ozone. *J. Geophys. Res.* 85, 3255–3263.

Kasting, J.F., Pollack, J.B., and Ackerman, T.P. (1984) Response of Earth's atmosphere to increases in solar flux and implications for loss of water from Venus. *Icarus* 57, 335–355.

Kasting, J.F., Whitmire, D.P., and Reynolds, R.T. (1993) Habitable zones around main sequence stars. *Icarus* 101, 108–128.

Kieffer, H.H., Martin, T.Z., Peterfreund, S.R., Jakosky, B.M., Miner, E.D., and Palluconi, F.D. (1977) Thermal and albedo mapping of Mars during the Viking primary mission. *J. Geophys. Res.* 82, 4249–4291.

Léger, A., Ollivier, M., Altwegg, K., and Woolf, N.J. (1999) Is the presence of H_2O and O_3 in an exoplanet a reliable signature of a biological activity? *Astron. Astrophys.* 341, 304–311.

Lindal, G.F., Wood, G.E., Hotz, H.B., Sweetnam, D.N., Eshelman, V.R., and Tyler, G.L. (1983) The atmosphere of Titan: an analysis of the Voyager 1 radio-occultation measurements. *Icarus* 53, 348–363.

Lunine, J.I. (1999a) *Earth: Evolution of a Habitable World*, Cambridge University Press, Cambridge.

Lunine, J.I. (1999b) Titan: a world seen but darkly. In *Our Worlds*, edited by A. Stern, Cambridge University Press, New York.

Lunine, J.I. (2001) The occurrence of Jovian planets and the habitability of planetary systems. *Proc. Natl. Acad. Sci. USA* 98, 809–814.

Morowitz, H.J. (1992) *Beginning of Cellular Life*, Yale University Press, New Haven, CT.

Owen, T. (1980) The search for early forms of life in other planetary systems: future possibilities afforded by spectroscopic techniques. In *Strategies for the Search for Life in the Universe*, edited by M. Papagianis, Reidel, Dordrecht, the Netherlands, pp. 177–185.

Reynolds, R.T., McKay, C.P., and Kasting, J.F. (1987) Europa, tidally heated oceans, and habitable zones around giant planets. *Adv. Space Res.* 7, 125–132.

Sagan, C., Thompson, W.R., Carlson, R., Gurnett, D., and Hord, C. (1993) A search for life on Earth from the Galileo spacecraft. *Nature* 365, 715–721.

Schneider, J. (1999) Extrasolar planets: detection methods, first discoveries and future perspectives. *C.R. Acad. Sci. Ser. 11B* 327(6), 621–634.

Schneider, J., Labeyrie, A. and Coliolo, F. (2000) A universal biosignature: generalized chlorophylls. In *2000 Spring Meeting, EOS Transactions*, American Geophysical Union, Washington, DC, Suppl. S30.

Seiff, A. (1983) Thermal structure of the atmosphere of Venus. In *Venus*, edited by D.M. Hunten, L. Colin, T.M. Donahue, and V.I. Moroz, University of Arizona Press, Tucson, pp. 215–279.

Selsis, F., Despois, D., and Parisot, J.-P. (2002) Signature of life on exoplanets: can Darwin produce false positive detections? *Astron. Astrophys.* 388, 985.

Tomasko, M.G. (1980) The thermal balance of Venus in light of the Pioneer Venus Mission. *Geophys. Res.* 85, 8187–8189.

Traub, W.A. and Jucks, K.W. (2002) A possible aeronomy of planetary systems beyond the solar system. In *Atmospheres in the Solar System: Comparative Aeronomy, AGU Geophysical Monograph 130*, edited by M. Mendillo, A. Nagy, and J.H. Waite, American Geophysical Union, Washington, DC, pp. 369–380.

Traub, W.A. and Stier, M.T. (1976) Theoretical atmospheric transmission in the mid-and far-infrared at four altitudes. *Appl. Optics* 15, 264–377.

Woolf, N.J., Smith, P.S., Traub, W.A., and Jucks, K.W. (2002) The spectrum of Earthshine: a pale blue dot observed from the ground. *Ap. J.* 574, 430.

Zahnle, K. (2001) Decline and fall of the Martian empire. *Nature* 412, 209–213.

Address reprint requests to:
David J. Des Marais
Ames Research Center
Moffett Field, CA 94035

E-mail: ddesmarais@mail.arc.nasa.gov